Chapter 2

The Viral Susceptibility of the *Haloferax* Species

Zaloa Aguirre Sourrouille[1*], Sabine Schwarzer[1,2*], Sebastian Lequime[3], Hanna M. Oksanen[4] and Tessa E.F. Quax[1,2]

***Contributed equally**

1 *Biology of Archaea and Viruses, Groningen Biomolecular Sciences and Biotechnology Institute, University of Groningen, 9747 AG Groningen, The Netherlands.*
2 *Archaeal Virus-Host Interactions, Faculty of Biology, University of Freiburg, Freiburg, Germany.*
3 *Cluster of Microbial Ecology, Groningen Institute for Evolutionary Life Sciences, University of Groningen, Groningen, the Netherlands.*
4 *Molecular and Integrative Biosciences Research Programme, Faculty of Biological and Environmental Sciences, University of Helsinki, Helsinki, Finland.*

Viruses. 2022 Jun 20. 14(6):1344.
doi: 10.3390/v14061344.

Abstract

Viruses can infect members of all three domains of life. However, little is known about viruses infecting archaea and the mechanisms that determine their host interactions are poorly understood. Investigations of molecular mechanisms of viral infection rely on genetically accessible virus-host model systems. Euryarchaea belonging to the genus *Haloferax* are interesting models, as a reliable genetic system and versatile microscopy methods are available. However, only one virus infecting the *Haloferax* species is currently available. In this study, we tested ~100 haloarchaeal virus isolates for their infectivity on 14 *Haloferax* strains. From this we identified 10 virus isolates in total capable of infecting *Haloferax* strains, which represented myovirus or siphovirus morphotypes. Surprisingly, the only susceptible strain of all 14 tested is *Haloferax gibbonsii* LR2-5, which serves as an auspicious host for all these 10 viruses. By applying comparative genomics, we shed light on factors determining host-range of haloarchaeal viruses on *Haloferax*. We anticipate our study to be a starting point in the study of haloarchaeal virus-host interactions.

Keywords: haloarchaea, archaeal virus, *Haloferax*, *Haloferax gibbonsii* LR2-5, host range

1 Introduction

Microbial viruses are widespread and able to infect members of all three domains of life, including archaea. Archaea are ubiquitous microorganisms that can be found in extreme environments, such as salt lakes, as well as in mesophilic surroundings, such as the oceans and the human body [1,2]. The study of archaeal viruses is essential to understand the origin and evolution of viruses in general [3]. Archaeal viruses display a high genomic and structural variability, but they also share some common traits with viruses infecting other domain of life [4-7]. Viruses are divided in different families, currently mainly based on the sequence similarities and the highest taxonomic ranks, realms, follow largely groupings based on the characteristics of virus major capsid proteins or genome replication components [5,8,9]. Whereas crenarchaeal viruses come in many different shapes, the majority of viruses infecting euryarchaea display a head-tail

morphology and are currently members of 14 families in the class *Caudoviricetes* [6,9-12]. The rest of the currently known euryarchaeal viruses are either internal membrane-containing tailless icosahedral (family *Sphaerolipoviridae*) [13], pleomorphic (family *Pleolipoviridae*) [14], or spindle-shaped (family *Halspiviridae*) [15]. Archaeal tailed viruses are the most common isolates infecting halophilic archaea. They are morphologically indistinguishable from tailed double-stranded (ds) DNA bacteriophages that have the myovirus (long and contractile helical tail), podovirus (short tails) or siphovirus (long and non-contractile tails) morphology. At the sequence level, however, archaeal tailed viruses are very diverse, several of them are singletons and they hardly resemble their bacterial relatives [10,16]. All isolated archaeal viruses have DNA genome so far and the majority of their genes encode proteins of unknown function showing limited or nonexistent similarity to tailed bacteriophage proteins, and as a result many aspects of archaeal virus-host relationships and virus life cycles remain unknown [6]. However, very recently, comparative genomics and host-range analysis of the tailed archaeal viruses showed the role of the tail fiber adhesin in host recognition [10]. The adhesins from archaeal viruses resemble the adhesins located at the distal tip of the tail fibers of various members of the T-even phage group [17]. The structural core of the adhesins is formed by highly conserved glycine-rich motifs that separate the hypervariable segments [17]. While these conserved glycine-rich domains are used for binding, mutations or shuffling of the hypervariable regions change adhesin receptor specificity and thus primarily determine the host range [10,18]. Previous screenings of haloarchaeal viruses and their hosts highlighted the high abundance of myovirus isolates and their extremely broad host ranges. The *Hafunaviridae* is the largest family of archaeal tailed viruses and its myoviruses have a broad host range [10,19]. Other haloarchaeal viruses are more specific to a certain host [10,18].

The study of the virus-host relationships and infection mechanisms of archaeal viruses would greatly benefit from the availability of genetically accessible virus-host models, for which molecular biology tools are available. For crenarchaeal virus hosts, several members of the genus *Sulfolobales* are currently the most common archaeal models with genetic systems available [20-24]. Moreover, there are already some genetic systems for crenarchaeal viruses available such as SSVs, STIV and STSV1 [25-28]. The study of euryarchaeal viruses presently relies mainly on haloarchaeal *Halorubrum* and *Haloarcula* strains that are infected by a substantial number of known viruses [10,19,29].

These hosts have been used successfully to study archaeal viruses and their structures, entry, and egress mechanisms [30-34]. However, the genetic and molecular toolset for these hosts is limited. In recent years, *Haloferax* has become increasingly popular in the archaeal scientific community, and it is the euryarchaeal model for which the most advanced tools for genetic engineering, imaging and molecular biology are available [35]. The *Haloferax* tools entail a versatile genetic system for overexpression and genomic knock-out, the availability of several plasmids and different markers and a CRISPR-based repression system to downregulate gene expression [23,36-39]. In addition, it is the only archaeon for which several fluorescent fusion proteins are available [40]. It is an excellent organism for light microscopy and is also used in microfluidics [40]. The development of these technical advances, and the growing scientific community embracing *Haloferax* as a central euryarchaeal model, has led to a substantial increase in the understanding of its cell biology [41-56].This detailed knowledge of euryarchaeal cell biology obtained using *Haloferax* as a model, is of great added value in studies of viral infection mechanisms.

In contrast to some other haloarchaea, there are far less viruses known that infect *Haloferax* straines. Almost 30 years ago, HF1 virus was reported to infect *Haloferax lucentense* and *Hfx. volcanii* and a defective provirus of *Haloferax mediterranei* has been identified, both of which are no longer available (M. Dyall-Smith, personal communication) [57,58]. At the moment, Haloferax tailed virus 1 (HFTV1) is only one virus isolated from a *Haloferax* host and its was recently isolated together with its host *Haloferax gibbonsii* LR2-5 from the hypersaline Lake Retba in Senegal [59,60].

Due to the attractiveness of *Haloferax* for molecular studies, we aim to identify viruses that infect *Haloferax* strains. In this study, we used the largest available collection of isolated and characterized haloarchaeal virus isolates and tested the infectivity of 95 viruses on 14 *Haloferax* strains. The virus collection contains viruses from all current haloarchaeal virus families, and these viruses represent the majority of haloarchaeal virus isolates isolated to date. This endeavor resulted in an extended virus-host matrix for *Haloferax*, from which we could identify a promising model that is the host to a substantial number of viruses, *Haloferax gibbonsii* LR2-5. In addition, we used comparative genomics to identify viral factors that allow infection of this *Haloferax* host. With this work we pave the way to using *Haloferax* as a model in virus-host interaction.

2 Materials and Methods

2.1 Archaeal Viruses and Strains and Growth Conditions

All *Haloferax* strains (Supplementary Table S1), virus host strains (Supplementary Table S2) and viruses (Supplementary Table S2) were grown aerobically at 37°C in modified growth medium (MGM) [58,61]. The artificial 30% salt water (SW) (240g NaCl, 30g$MgCl_2$ × 6H_2O, 35g$MgSO_4$ × 7H_2O, 7gKCl, 5mL of 1M$CaCl_2$ × 2H_2O and 80mL of 1 M Tris-HCl, pH 7.2 per liter) was diluted to obtain 18, 20, or 23% SW in the top-agar media, plates, and liquid media, respectively. MGM also contained 5 g of peptone (Oxoid), 1g of Bacto yeast extract (Becton, Dickinson and Company, Sparks, MD, USA) and Bacto agar (14g for plates; 4g per top-layer; Becton, Dickinson and Company) per liter. Viruses were grown on their own host strain listed in Table S2 S2 by using double-layer plaque assay. For plaque assays, the strains were grown 2–3 over nights in liquid media to obtain a dense culture (OD ~1) of which 200–300µl were used per plate for inoculation to obtain an even layer of dense growth of the strain on a soft agar layer. Viruses diluted in MGM broth were added 100µl per plate. The virus and strain were combined with melted soft agar (3–4mL per plate; 50°C), mixed and plated. The plates were grown for 2–4 days in a box (in some cases with an additional cup of water) to prevent them from drying out. The plaques observed on plates were used to enumerate the viruses in the samples by taking into account the virus dilution and plates with confluent or semi-confluent growth of virus were used to produce virus lysates. Virus lysates were prepared by mixing the collected soft agar layer from confluent or semi-confluent plates with 2–3ml of MGM broth per plate. After 1.5 h of shaking at 37°C, lysates were cleared from cell debris and agar by centrifugation (Sorvall F14 rotor, 10 000rpm, 20min, 4°C). Lysates were stored at +4°C for up 2 months before use.

2.2 Sensitivity of Haloferax Strains to Euryarchaeal Viruses

The sensitivity of *Haloferax* strains (Supplementary Table S1) to viruses (Supplementary Table S2) was determined by placing 10µl drops of undiluted and 1:100 diluted virus lysates applied to *Haloferax* strain plated with top-agar on a plate using double-layer plaque assay. The host strains of the viruses (Supplementary Table S2) were used as positive controls. For virus drops, MGM was used as negative control. The drops were repeated in duplicate. All cases where cell growth was inhibited on a plate in the presence

of virus lysate, were further tested by double layer plaque assay to confirm viral infection and obtain numerical values of efficiency of infection. All titer data was collected at 37°C.

2.3 Viral Comparative Genomics

The genomic sequences of the viruses were retrieved from NCBI [62]. Phylogenetic trees were constructed using a custom-written R script with the package ggtree [63] using the ANI values calculated with VIRIDIC [64]. Whole genome sequence alignments were visualized with Easyfig [65]. To find putative virus-host determinants protein sequences found at variable regions of the viral genomes were downloaded from NCBI and aligned using MAFFT v. 7.450 with default settings [66] and visualized by Jalview. Under-represented tetramers were detected using https://www.cmbl.uga.edu//software/signature.html and for more complex motifs a manual search was carried out in Geneious v 8.1.9.

The phylogenetic analyses of the adhesin and tail fiber gene sequences were carried out as follow. For both datasets sequences were aligned using MAFFT v. 7.450 [66], and a maximum-likelihood phylogenetic tree constructed with IQ-TREE v. 1.6.12 [67], using ModelFinder for model selection [68]. Additional phylogenetic analyses were conducted in BEAST 1.10.4 [69], using the best nucleotide substitution model as determined in ModelFinder and available in BEAST, namely WAG+F+G4 [70] and BLOSUM62+F+G4 [71] for the adhesins and tail fibers gene sequences, respectively. All sequences were considered isochronous, and the evolutionary process was reconstructed under a strict molecular clock with a fixed rate of 1 and a constant population size model [72]. The infection capability of the LR2-5 strain was considered as a discrete trait analyzed using a symmetric diffusion model [73], and the number of changes between the two states (Markov jumps) was estimated in the posterior distribution of trees [74]. Proper convergence and mixing (effective sample size>200) was verified using tracer v. 1.7 [75] and the burn-in (10% of samples) was removed. The presence of a phylogenetic signal linked to the LR2-5 infection capability was tested by comparing the distribution of Markov jumps to a "null distribution" of estimated number of Markov jumps computed by a set of 10 independent runs, where the states (i.e., LR2-5 infection capability) were randomized. A clear overlap between the 95% highest posterior density (95% HPD) of the estimated number of Markov jumps in the original dataset and the randomized "null" distributions would sign the absence of a phylogenetic signal [73]. If not otherwise stated, default parameters were used.

3 Results and Discussion

3.1 Detection of Viruses Infecting Haloferax Strains

To identify novel virus-host models for *Haloferax*, a collection of 95 haloarchaeal viruses (Supplementary Table S2) were cross-tested with 14 *Haloferax* strains (Supplementary Table S1, Figure 1). The viruses have been isolated from samples taken from different hypersaline environments and are part of the collection at the University of Helsinki. Information on the origins, host strains, virus morphologies, genomes, and taxonomic classification of the viruses can be found in Supplementary Table S2. Some of the 14 tested *Haloferax* strains are widely used laboratory models, such as *Hfx. volcanii* H26 and *Hfx. mediterranei* [76], while several other strains were isolated quite recently from the hypersaline Lake Retba in Senegal (Supplementary Table S2) [59]. A scheme of the experimental pipeline for the screening is depicted in Figure 1.

The screening resulted in the detection of 10 virus isolates that could make plaques on *Haloferax* strains tested (Table 1). Curiously, *Hfx. gibbonsii* LR2-5 was the only susceptible *Haloferax* strain. The LR2-5 infecting viruses belong to the genera *Haloferacalesvirus*, *Mincapvirus* (family *Hafunaviridae*) or *Retbasiphovirus* (family *Haloferuviridae*) (Table 1). It is important to note that during the course of the study, HCTV-6 and HCTV-13 genome sequences were reported to be identical [10] and as a result, nine unique virus isolates infecting *Haloferax* strains were identified. Furthermore, the infectivity of the closely related virus isolates assigned to the three genera were re-tested with LR2-5 by plaque assay, but no more interactions were detected (Table 1).

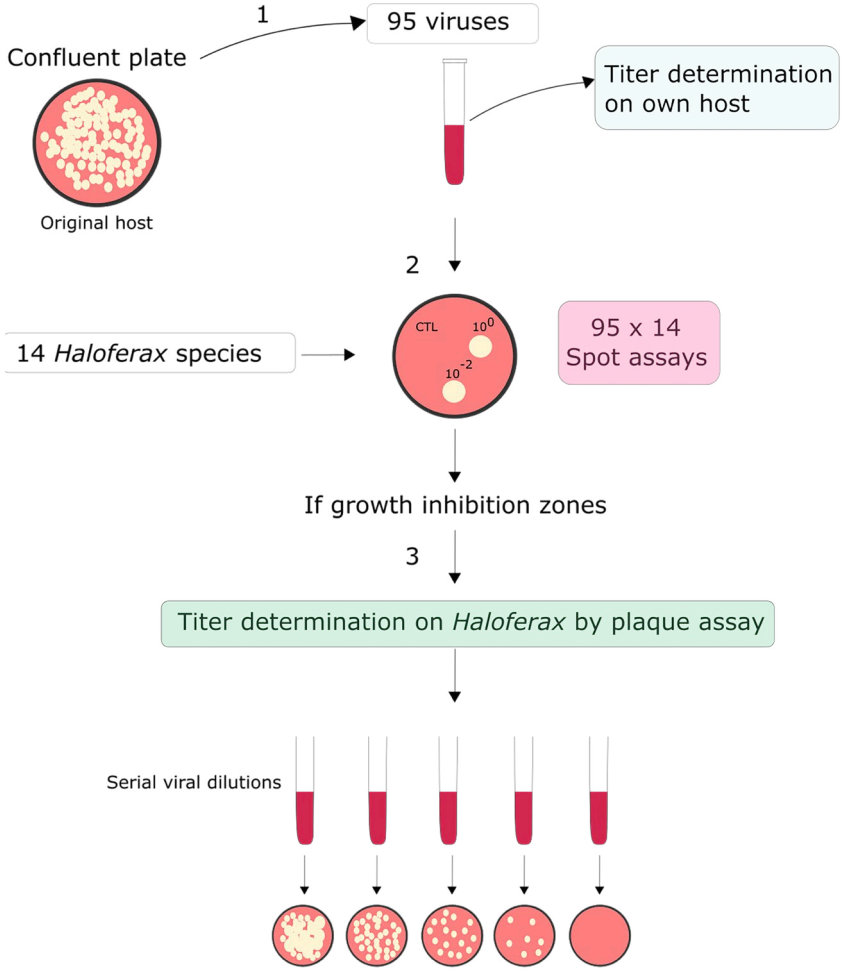

Figure 1. A schematic overview of the virus-host screen. Step 1: Fresh virus stocks made from confluent or semi-confluent plates were prepared on their own host strains and the titers were determined on their own host strains. **Step 2:** 95 virus stocks (undiluted and 10^{-2} dilution) were spotted on lawns of 14 *Haloferax* strains. MGM medium was used as a negative control (CTL). **Step 3:** After incubation at 37°C, all virus-*Haloferax* pairs that resulted in growth inhibition on the spot-on lawn-assay were further tested by plaque assay by making serial dilutions of the virus stock and plating with the *Haloferax* strains to be tested. Viral plaques observed on *Haloferax* were counted, the titers were determined and positive virus-*Haloferax* pairs were noted in Table 1.

Table 1. ***Haloferax gibbonsii*** **LR2-5 infecting viruses and the closely related virus isolates assigned to same genus**

Virus	Virus morphology [5]	Host strain to grow the virus	Titer on own host, pfu/ml	Titer on LR2-5, pfu/ml	EOP on LR2-5[6]
Hafunaviridae (F) [1]					
Haloferacalesvirus (G) [2]					
HRTV-10	M	*Halorubrum* sp. B2-2	1.2×10^{9}	6.8×10^{3}	6×10^{-6}
HRTV-18	M	*Halorubrum* sp. SS10-3	7.5×10^{9}	-	
HRTV-20	M	*Halorubrum* sp. SS10-9	7.0×10^{10}	-	
HRTV-22	M	*Halorubrum* sp. SS10-9	1.1×10^{10}	-	
HRTV-26	M	*Halorubrum* sp. SS10-9	1.4×10^{9}	4.3×10^{6}	3×10^{-3}
HRTV-5	M	*Halorubrum* sp. s5a-3	2.0×10^{10}	-	
HCTV-7 [3]	M	*Haloarcula californiae*	4.8×10^{10}	-	
[HCTV-12] [3]	M	*Haloarcula californiae*	1.3×10^{10}	-	
HCTV-9	M	*Haloarcula californiae*	2.8×10^{10}	-	
HCTV-11	M	*Haloarcula californiae*	4.0×10^{10}	-	
HRTV-9	M	*Halorubrum* sp. B2-2	5.3×10^{9}	-	
HRTV-16	M	*Haloterrigena* sp. SS13-7	nd	nd	
HCTV-8	M	*Haloarcula californiae*	2.3×10^{10}	3.1×10^{5}	1×10^{-5}
HCTV-10	M	*Halorubrum sodomense*	2.3×10^{9}	-	
HJTV-1	M	*Haloarcula japonica*	1.6×10^{9}	-	
HRTV-13	M	*Halorubrum* sp. SS8-2	5.1×10^{9}	-	
HRTV-21	M	*Halorubrum* sp. SS10-9	2.8×10^{9}	-	
Mincapvirus (G) [2]					
HSTV-2	M	*Halorubrum sodomense*	8.2×10^{9}	2.3×10^{10}	3
HRTV-7	M	*Halorubrum* sp. B2-2	2.1×10^{9}	7.9×10^{5}	4×10^{-4}
HRTV-2	M	*Halorubrum* sp. s1-2	2.0×10^{10}	4.6×10^{10}	2
HRTV-11	M	*Halorubrum* sp. SL-5	4.7×10^{10}	-	
HCTV-6 [4]	M	*Haloarcula californiae*	1.6×10^{10}	3.9×10^{9}	2×10^{-1}
[HCTV-13] [4]	M	*Haloarcula californiae*	2.5×10^{9}	[1.3×10^{7}]	[5×10^{-3}]
HCTV-15	M	*Halorubrum* sp. SS6-2	1.9×10^{10}	9.6×10^{6}	5×10^{-4}
Haloferuviridae (F) [1]					
Retbasiphovirus (G) [2]					
HFTV1	S	*Haloferax gibbonsii* LR2-5	2.9×10^{12}	2.9×10^{12}	1

[1]Family; [2]Genus; [3]HCTV-7 and HCTV-12 are identical and both tested here; HCTV-7 will be used in future; [4]HCTV-6 and HCTV-13 are identical and both tested here; HCTV-6 in used in future; [5]S, siphovirus morphology; M, myovirus morphology; [6]Relative efficiency of plating (EOP) on LR2-5 compared to the own host with an EOP of 1.

In several cases, however, we observed a growth inhibition zone by spot-on-lawn assay but no plaques during the plaque assay (Table S2). As haloarchaea are known to produce antimicrobial toxins i.e. halocins [77,78], we assume that halocins produced by the virus host cell are present in some of the virus stocks. These halocins would result in a growth inhibition in spot-on-lawn assays but will not result in plaques. Only those virus-host pairs for which plaques were detected, were marked as positive and true virus-host pairs. The quantitative plaque assay also allowed to determine the viral titer on the *Haloferax* host, which is an indication of the efficiency of infection. As a summary, we did not find any true virus-host pairs on any of the *Haloferax* strains, except on strain *Haloferax gibbonsii* LR2-5, which was isolated a few years ago from Lake Retba in Senegal at the same time as HFTV1 [59,60]. All LR2-5 infecting viruses had either *Halorubrum* or *Haloarcula* as their own host and their titers varied between 10^3 and 10^{10}PFU/ml on LR2-5 (Table 1). On the other hand, we also calculated the efficiency of plating (EOP) of the viruses that were able to infect LR2-5 to compare them with their original isolation host. The efficiency of plating (EOP) of three mincapviruses HSTV-2, HRTV-2, and HCTV-6 originally grown either on *Halorubrum* or *Haloarcula* hosts had slightly higher or around same EOP on LR2-5 than on their own host. However, rest of the LR2-5 infecting viruses had three to six magnitudes lower EOPs on LR2-5 than on their own host. These results are in accordance with previous observations, which showed that myoviruses infecting halophilic archaea have a wide host range [10,78].

3.2 Characteristics of Haloferax Infecting Viruses

To map the determinants of viral host range, we focused on viruses that infect LR2-5 and those viruses belonging to the same genus as LR2-5 infecting viruses (genera *Haloferacalesvirus*, *Mincapvirus*, *Retbasiphovirus*; Table 1). A phylogenetic tree based on the complete genome sequences of the haloferacalesviruses, mincapviruses and retbasiphovirus (Figure 2) and their EOPs on LR2-5 (Table 1) revealed that all mincapviruses, except HRTV-11, can infect LR2-5.

The LR2-5 infecting viruses have been isolated from hypersaline environmental samples either from Israel, Italy, Senegal, Slovenia, or Thailand (Figure 3A, Supplementary Table S2). All viruses represented tailed morphologies (Table 1). HFTV1 is the only siphovirus and the rest of the LR2-5 infecting viruses are myoviruses (Table 1). A schematic of the morphologies and a typical genome organization of myovirus and siphovirus are shown in Figure 3B.

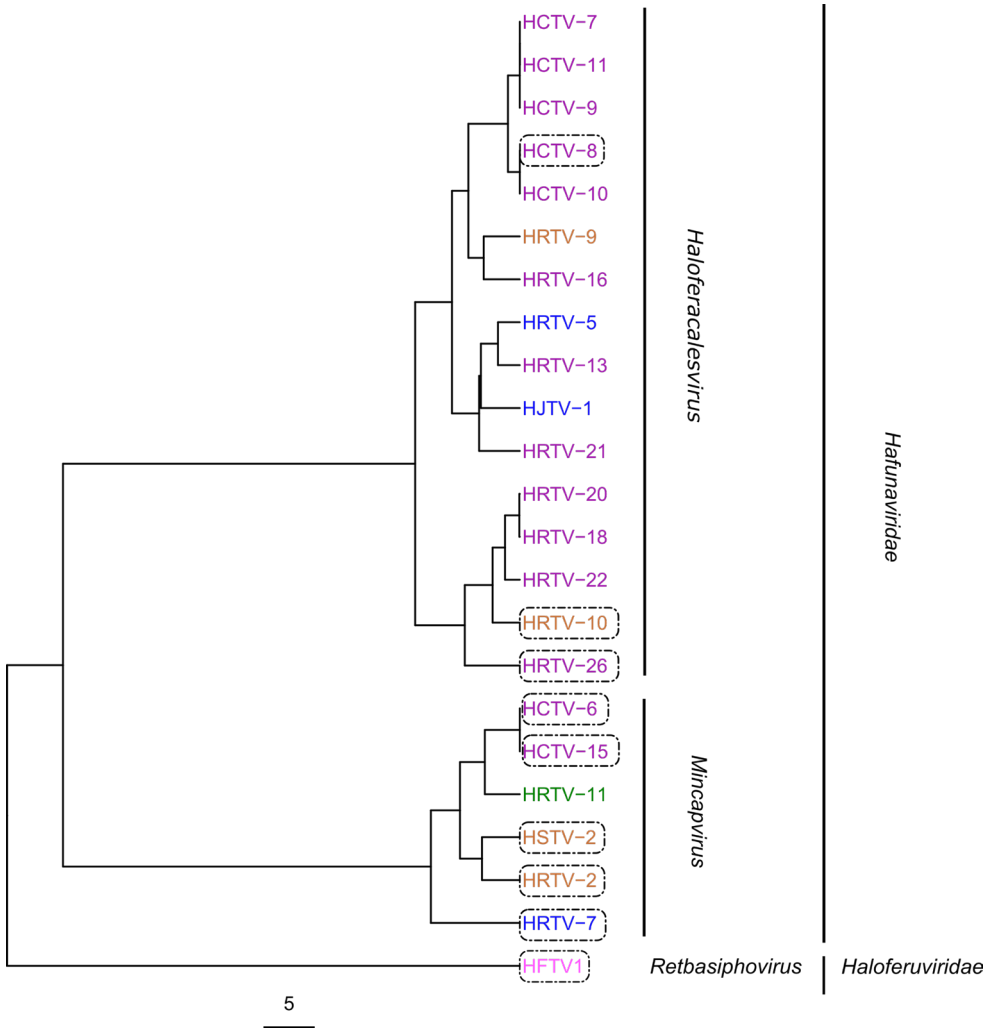

Figure 2. Phylogenetic tree of viruses belonging to the *Haloferuviridae* and *Hafunaviridae* families based on average nucleotide identity (ANI) values calculated using the VIRIDIC software. Viruses infecting LR2-5 are surrounded by a box. All nodes are supported above 75% except the one indicated with *. Scale bar represents the number of substitutions per nucleotide position. Place of isolation: pink Senegal, purple Thailand, green Slovenia, orange Israel, blue Italy.

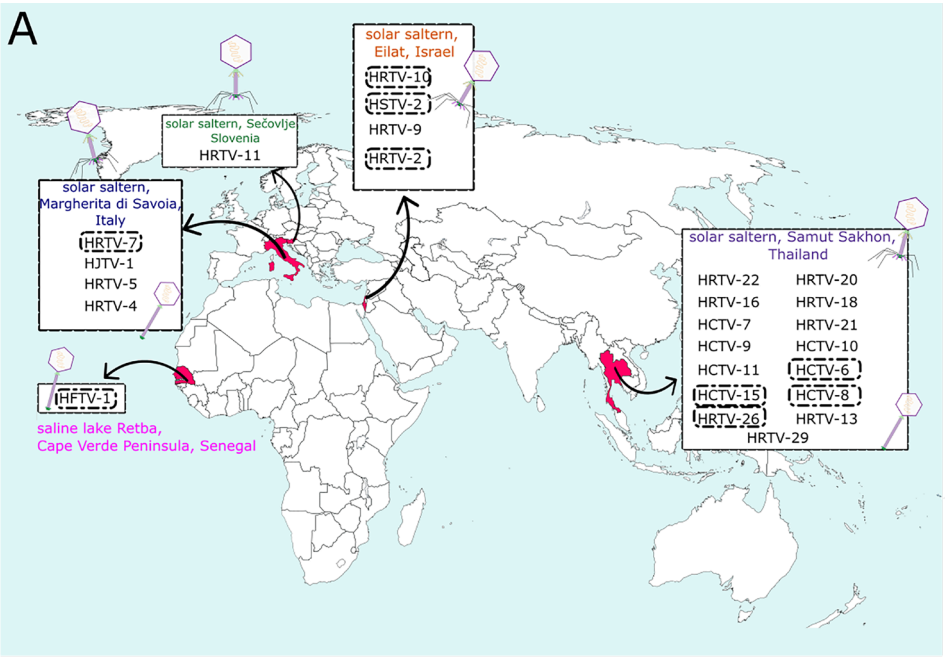
A
solar saltern, Eilat, Israel
HRTV-10
HSTV-2
HRTV-9
HRTV-2
solar saltern, Sečovlje Slovenia
HRTV-11
solar saltern, Margherita di Savoia, Italy
HRTV-7
HJTV-1
HRTV-5
HRTV-4
HFTV-1
saline lake Retba, Cape Verde Peninsula, Senegal
solar saltern, Samut Sakhon, Thailand
HRTV-22
HRTV-20
HRTV-16
HRTV-18
HCTV-7
HRTV-21
HCTV-9
HCTV-10
HCTV-11
HCTV-6
HCTV-15
HCTV-8
HRTV-26
HRTV-13
HRTV-29

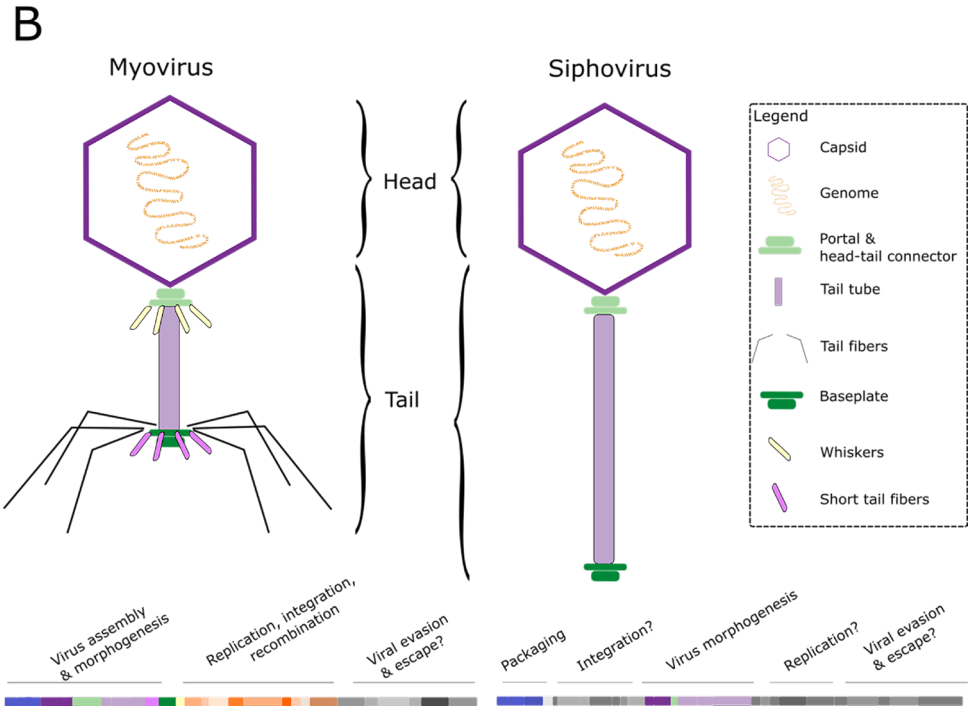
B
Myovirus
Siphovirus
Head
Tail
Legend
Capsid
Genome
Portal & head-tail connector
Tail tube
Tail fibers
Baseplate
Whiskers
Short tail fibers
Virus assembly & morphogenesis
Replication, integration, recombination
Viral evasion & escape?
Packaging
Integration?
Virus morphogenesis
Replication?
Viral evasion & escape?

Figure 3. (A) Isolation sites of the haloferacalesviruses, mincapviruses and retbasiphovirus (see also Supplementary Table S2). Schemes of the viral morphologies that were observed in each group are also indicated (see also Table 1). LR2-5 infecting viruses are circled with a dash line. **(B)** Schematic representation of the myovirus and siphovirus virion morphologies (not in scale) and a typical genome organization consisting of different functional modules of tailed archaeal viruses.

HRTV-11 is the only mincapvirus isolated from a remote location, Slovenia, where no other haloarchaeal virus were successfully isolated (Figure 3A; [29]) . The broad host range of myoviruses has been linked to their ability to exchange their host-specific genetic modules for receptor binding proteins [19]. Thus, we hypothesize that the host range of viruses isolated from locations with a low virus-density might be different from other closely related viruses, isolate from virus-dense environments, as the possibility for recombination events might have been limited We had a closer look into possible host-range determining factors, to find potential explanations for the few haloferacalesviruses that exceptionally do infect LR2-5.

3.3 Restriction-Modification Systems

Viruses are known to develop strategies to escape host defense mechanisms. Thus, we explored in more detail the antiviral-defense mechanisms of the host and the viral escape mechanisms to determine if any of these factors could explain the differences in the ability to infect LR2-5 between viruses from the same family. LR2-5 does not have a CRISPR-cas system, but encodes a predicted type I restriction modification (RM) system [60]. These antiviral mechanisms are based on methylation of host DNA (to protect it) and cleavage of unmethylated DNA (viral DNA). Part of the LR2-5 encoded RM system are a Zim methylase (CTAG methyltransferase), Mrr-like endonuclease and RmeRMS (type I restriction enzyme restriction/methylation/specificity subunit).

One strategy of viruses to escape host recognition is the avoidance of certain motifs in their genomes, which are the targets for the RM systems [79]. In line with previous studies [79], the palindromic tetrameric motifs CTAG, GATC and AGCT are absent in the mincapvirus genomes, whereas haloferacalesviruses lack only CTAG and GATC, except of HRTV-22 which contains a CTAG motif (Supplementary Table S3). Furthermore, mincapviruses and haloferacalesviruses show an underrepresentation of the TGCA and CATG motifs. On the other hand, those tetrameric motifs are also under-represented

in the genomes of haloferuviruses (Supplementary Table S3). We did not observe any differences between the viruses with respect to underrepresented motifs, which would be able to explain different infectivity of the studied viruses on LR2-5.

Methylated motifs in the genome of LR2-5 were previously predicted [60]. We searched for sequences in viral genomes that might be recognized by the host methyltransferases. We hypothesize that when the viral genome is replicated the host will recognize those sequences as "self" and methylate the viral DNA, hence, allowing the virus to escape the antiviral-mechanism. Calculation of the frequency of corresponding motifs in the viral genomes revealed that the motif GCGCTG is found more frequently in all mincapviruses than in haloferacalesviruses (Supplementary Table S4). The frequency of the other motifs was similar for all viruses. Therefore, we concluded that host range determinants in case of LR2-5 infecting viruses might rely on another factor.

3.4 Adhesins and Tail Fiber Proteins

Pairwise alignment of the viral genomes of the *Hafunaviridae* family members showed the same genome organization within their own group (mincap- or haloferacalesviruses) (Figure 4). There were only a few variable genomic regions observed. Firstly, at the right-end of the genomes a region was detected with frequent insertions and inversions (Figure 4). Many of the proteins encoded by genes in this region are designated as hypothetical and they lack homology with proteins found in reference databases. It might be possible that these genes encode proteins involved in viral egress, as several of them have predicted transmembrane domains. However, since egress mechanisms of haloarchaeal viruses are not well understood, and the responsible proteins are not identified, it is not clear if these genes are determinants of differences observed in viral infectivity on LR2-5.

Figure 4. Schematic genomic alignment of the (A) mincapviruses, and (B) haloferacalesviruses. Grey bars represent homologous genomic regions. The level of nucleotide identity is reflected by the intensity of grey. Genes encoding major capsid protein (orange) and adhesins (pink) are indicated. The LR2-5 infecting viruses are circled with dashed lines. Identical or very similar genomes are shown as one and virus names are separated by /. Figures are prepared with Easyfig.

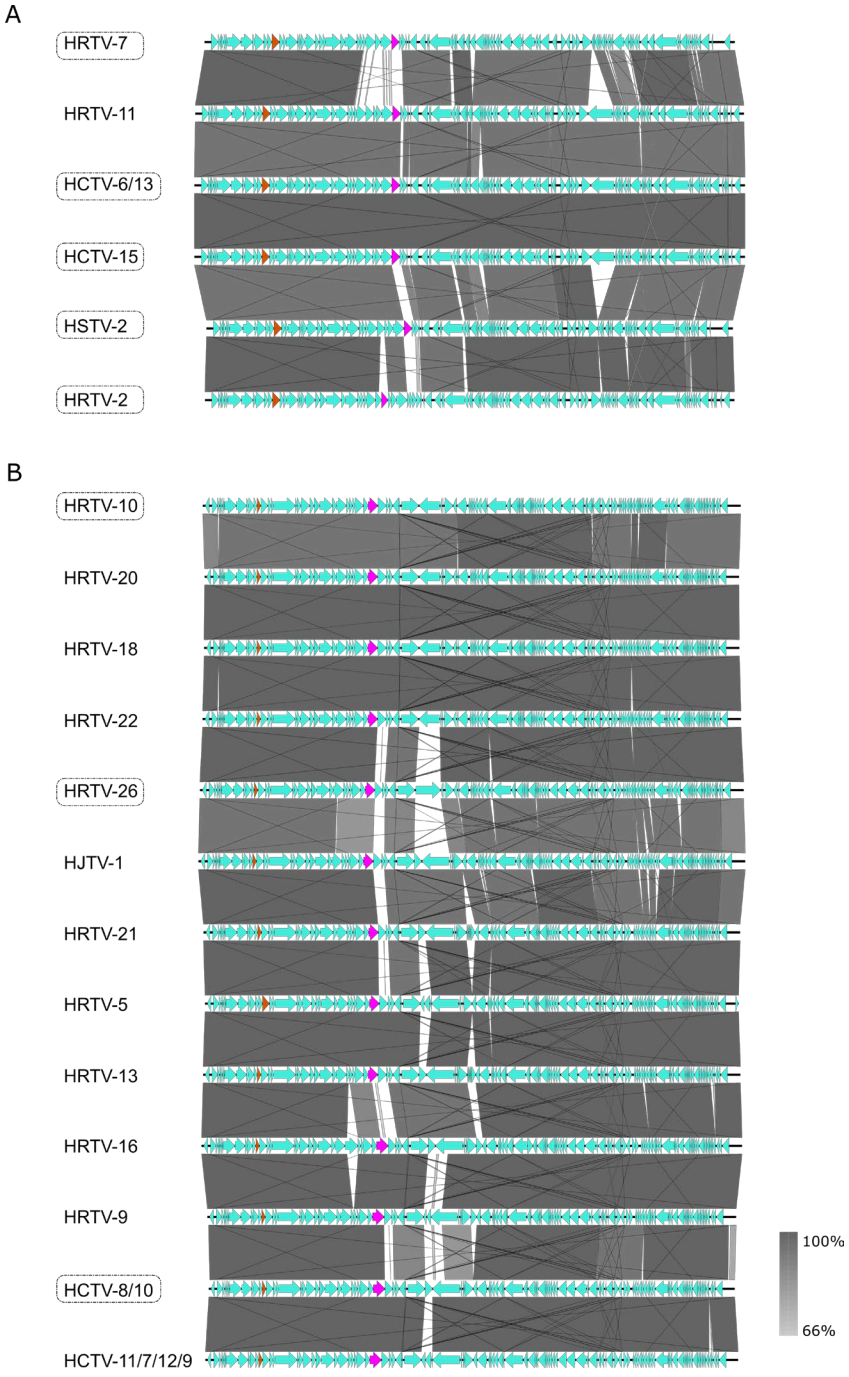
A
HRTV-7
HRTV-11
HCTV-6/13
HCTV-15
HSTV-2
HRTV-2
B
HRTV-10
HRTV-20
HRTV-18
HRTV-22
HRTV-26
HJTV-1
HRTV-21
HRTV-5
HRTV-13
HRTV-16
HRTV-9
HCTV-8/10
HCTV-11/7/12/9
100%
66%

Another highly variable region in the viral genomes is located around genes encoding the viral tail fiber and adhesin (Figures 4 and 5). Adhesins, located at the distal tip of the tail fibers, have been shown to be the host determinants in the tailed dsDNA bacteriophages of the order *Caudoviricetes* [17]. Long tail fibers of bacteriophages have a modular organization and consist of several different proteins [18,80]. Moreover, it has been suggested that haloarchaeal tailed viruses exchange the genes encoding either the tail fiber or adhesin with other viruses by recombination [10]. All haloferacalesviruses and mincapviruses have a gene encoding for a putative tail fiber protein together with a gene encoding a putative adhesin [10]. HFTV1 a siphovirus with a long non-contractile tail and does not contain tail fibers.

A tree of the hafunaviruses (haloferacalesviruses and mincapviruses) tail fiber adhesin proteins showed that they are divided in four clades (Figure 5) as also shown by Liu et al. [10]. Clade 1 and Clade 3 adhesins were previously reported to correlate well with the observed virus host range among the tested *Haloarcula*, *Halobacterium*, *Halobellus*, *Halorubrum*, and *Haloterrigena* strains [10]. We aimed to test if this correlation between adhesins and host range could also be seen in our current data set.

We investigated the hypothetical relationship between the susceptibility of the LR2-5 strain to infection and diversification of the hafunavirus tail fiber and adhesin genes by comparing the number of Markov jumps (i.e., infecting or not LR2-5) through the adhesin and the tail fiber gene evolution (Figure 5). A "null" distribution for each gene was generated by randomizing the state's distribution. We observed a clear overlap between the estimated numbers of Markov jumps (95% highest posterior density; HPD) in the real and randomized datasets, indicating a lack of phylogenetic signal linked to the viral infection capability on LR2-5 strain for both hafunavirus tail fiber gene and adhesin gene (Figure 5).

Based on this analysis, we d id not observe any clear correlation between the type of adhesin or tail fiber gene and the viral ability to infect *Hfx. gibbonsii* LR2-5. However, it should be emphasized that our dataset is limited to *Haloferax* hosts. Such a correlation between host range and adhesin type might only become apparent when a more diverse set of hosts is used, as the *Haloferax* strains are generally not very susceptible for viral infection. However, we did find a few case examples, which seems to pinpoint the adhesin as host determining factor. First, HRTV-26, one of the few haloferacalesviruses that is infecting LR2-5, encodes a Clade 1 adhesin, just like most mincapviruses. Since

the adhesins of haloferacalesviruses that are closely related to HRTV-26 all belong to Clade 3, it is likely that HRTV-26 picked up an adhesin gene via horizontal gene transfer from one of the Clade 1 viruses. This might be the explanation, why HRTV-26, even though it is an haloferacalesvirus, is still capable of infecting LR2-5.

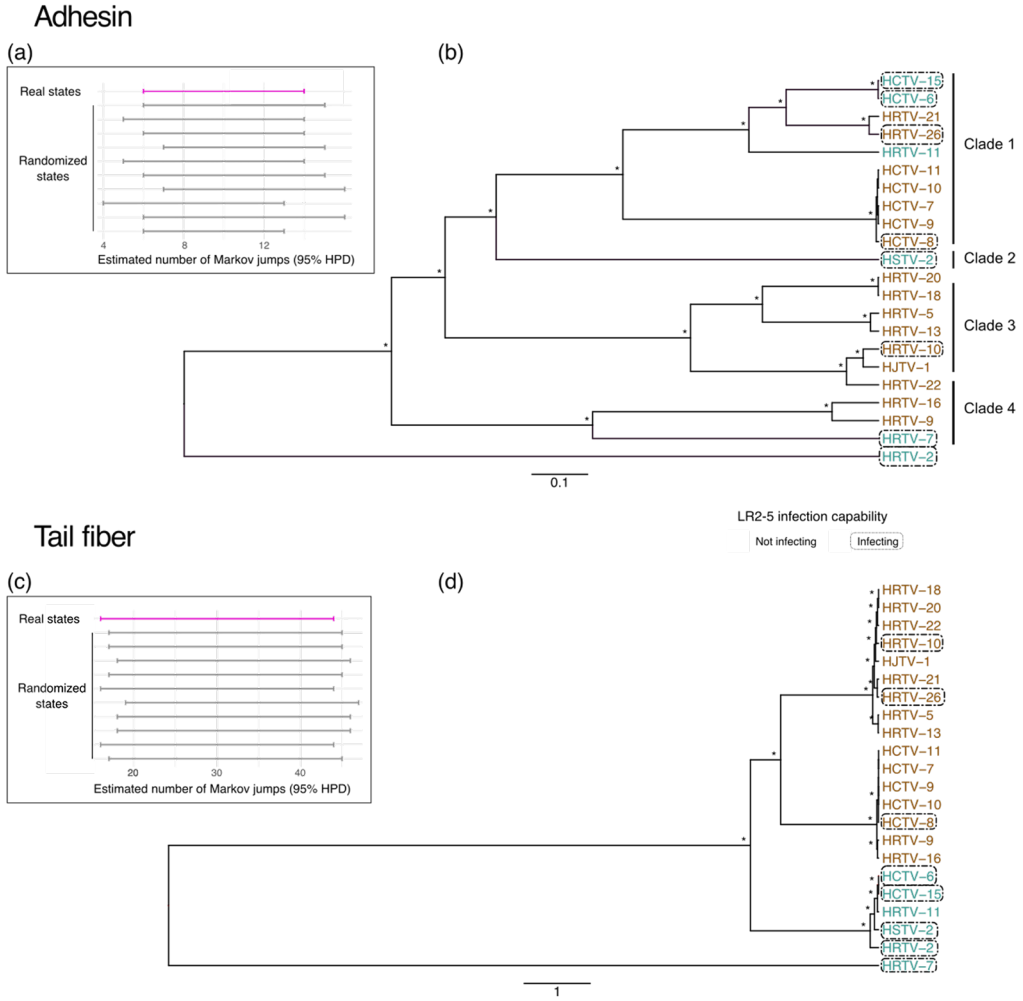

Figure 5. Comparison of the adhesin and tail fiber gene sequence phylogenies to the ability of viruses to infect LR2-5. (a) and **(c)** Distribution of Markov jumps (95% HPD) for (i) real states (pink) and (ii) randomized states (grey). **(b)** and **(d)** Bayesian maximum clade credibility tree with discrete trait reconstruction based on adhesin or tail fiber gene sequences respectively. Asterisk indicates node posterior probabilities higher than 0.8, and viruses in the boxes can infect LR2-5. Color code indicates the genus; blue *Mincapvirus*, brown *Haloferacalesvirus*.

Second, viruses encoding a Clade 3 adhesin do not infect LR2-5, with the exception of HRTV-10. To gain more insight into the HRTV-10 tail fiber adhesin, a multiple sequence alignment was performed. We identified one mutated codon resulting in an amino acid change (T380A) in a conserved motif at the 3'end of the adhesin gene (Supplementary Figure S2). This subtle substitution might be a possible explanation for its increased infectivity on LR2-5 as this could produce alterations in the fold and topology of adhesins. Liu et al. [10] already discussed how a single amino acid substitution (A217V) in the adhesins of HRTV-19 and HRTV-23 alters the host range. Moreover, Trojet et al. [17] showed how the long tail fiber locus in the T4 superfamily viruses is susceptible to frequent modular shuffling, which results in chimeric adhesins and, thus, viruses acquire new host receptor specificities. However, this hypothesis requires further experiments.

4 Conclusions

We aimed to develop an euryarchaeal virus-host model system with attractive molecular, genetic and imaging tools to dive deeper into virus-host relationships in archaea. We focused on *Haloferax* strains, as for these organisms the most advanced molecular and genetic tools are available. Due to the low number of known viruses that infect *Haloferax*, we set up a large-scale assay to identify viruses capable of infecting *Haloferax* strains. Our extensive screening of around 100 isolated and mostly characterized haloarchaeal viruses, showed that only a small subset was capable of infecting *Haloferax*. Specifically, *Hfx. gibbonsii* LR2-5 showed itself as an auspicious host, as we identified 10 virus isolates that can infect this host and all other hosts could not be infected. Previously, we have studied potential factors that make *Hfx. gibbonsii* LR2-5 (DSM No. 112399) so much more receptive to virus infection in contrast to related strains. For its virus susceptibility several possible factors were identified as potential explanations. The most prominent is an absence of CRISPR-cas virus defense systems in LR2-5 [60]. In addition, *Hfx. gibbonsii* LR2-5 has a different RM system from some other *Haloferax* strains, and the cell surface might show a different composition than that of other *Haloferax* strains, because LR2-5 encodes divergent surface proteins that might serve as viral receptors, such as pili and S-layer proteins [60]. These latter two proteins are a common component of the archaeal cell-surface and hypothesized to be used by viruses for initial binding and recognition [81,82].

Because we used plaque assays for the host-range determination, we cannot distinguish at which step of the infection cycle viruses are not successful in infecting a host: entry, replication or release. However, the results of the present study might indicate that adhesins, which are required for entry, are an important factor determining host range specificity, whereas other factors such as the viral egress proteins and restriction modification systems might also play a role. Moreover, it should be noted that one limitation of the approach utilized is the assumption that the successful infection of the host results in plaque formation. It could be that some of the viruses studied here might have integrated their genome when infecting *Hfx. gibbonsii* LR2-5, and, transferred to a lysogenic cycle. Consequently, these types of interactions would not show clear plaques and could have been missed by our approach. However, further experimental research on the implications of these proteins in host range is needed.

Our analysis has identified *Hfx. gibbonsii* LR2-5 as the only virus susceptible *Haloferax* strain. This host can be infected by 10 different viruses with sequenced genomes [10,16], and thus offers the possibility to compare infection mechanisms between viruses. Moreover, its genome is sequenced and its cell biology is characterized [60]. We are also currently developing a genetic system based on PyrE for *Hfx. gibbonsii* LR2-5. We conclude that this species is an extremely promising model host to study virus-host interactions in haloarchaea and anticipate that this work serves as a stepping stone for future in-depth molecular characterization of archaeal viral infection mechanisms.

Supplementary Materials: The following supporting information can be downloaded at: https://www.mdpi.com/article/10.3390/v14061344/s1, Table S1. Haloferax strains used in the study [19,29,37,59,60,76]; Table S2. Viruses used in the study; Table S3. Underrepresented palindromic motifs in viral genomes; Table S4. Manual counting of modified DNA motifs found in the genomes of viruses infecting Hfx. gibbonsii LR2-5; Figure S1. Multiple sequence alignment of adhesins belonging to the Group 3, Figure S2. VIRIDIC generated heatmap.

Author Contributions: T.E.F.Q. and H.M.O. conceptualized the research. T.E.F.Q., H.M.O, Z.A. and S.S. planned experiments and interpreted data. Z.A. and S.S. performed experiments. Z.A. and S.L. performed comparative genomics. All authors contributed to the writing of the paper. All authors have read and agreed to the published version of the manuscript.

Funding: This research was supported by funding from the Hector Fellow Academy to T.E.F.Q. and Z.A., an Emmy Noether grant (411069969) of the DFG to T.E.F.Q. and by the University of Helsinki and Academy of Finland funding for FINStruct and Instruct-FI, part of Biocenter Finland and Instruct-ERIC, respectively.

Institutional Review Board Statement: Not applicable.

Informed Consent Statement: Not applicable.

Data Availability Statement: The data presented in this study are available within the article and its Supplementary Materials.

Acknowledgments: We would like to thank Sari Korhonen, Xueting Wang and Zhengqun Li for practical support of the virus-host screen and M. Dyall-Smith for advice on the comparative genomics.

Conflicts of Interest: The authors declare no conflict of interest.

References

1. Borrel, G.; Brugère, J.F.; Gribaldo, S.; Schmitz, R.A.; Moissl-Eichinger, C. The Host-Associated Archaeome. *Nat. Rev. Microbiol.* 2020, *18*, 622–636.
2. Lloyd, K.G.; May, M.K.; Kevorkian, R.T.; Steen, A.D. Meta-Analysis of Quantification Methods Shows That Archaea and Bacteria Have Similar Abundances in the Subseafloor. *Appl. Environ. Microbiol.* **2013**, *79*, 7790–7799, doi:10.1128/AEM.02090-13.
3. Forterre, P.; Prangishvili, D. The Origin of Viruses. *Res. Microbiol.* **2009**, *160*, 466–472, doi:10.1016/j.resmic.2009.07.008.
4. Hartman, R.; Munson-McGee, J.; Young, M.J.; Lawrence, C.M. Survey of High-Resolution Archaeal Virus Structures. *Curr. Opin. Virol.* 2019, *36*, 74–83.
5. Baquero, D.P.; Liu, Y.; Wang, F.; Egelman, E.H.; Prangishvili, D.; Krupovic, M. Structure and Assembly of Archaeal Viruses. In *Advances in Virus Research*; Academic Press Inc., 2020; Vol. 108, pp. 127–164 ISBN 9780128207611.
6. Prangishvili, D.; Bamford, D.H.; Forterre, P.; Iranzo, J.; Koonin, E. V.; Krupovic, M. The Enigmatic Archaeal Virosphere. *Nat. Rev. Microbiol.* **2017**, *15*, 724–739, doi:10.1038/nrmicro.2017.125.
7. Pietilä, M.K.; Demina, T.A.; Atanasova, N.S.; Oksanen, H.M.; Bamford, D.H. Archaeal Viruses and Bacteriophages: Comparisons and Contrasts. *Trends Microbiol.* **2014**, *22*, 334–344, doi:10.1016/j.tim.2014.02.007.
8. Abrescia, N.G.A.; Bamford, D.H.; Grimes, J.M.; Stuart, D.I. Structure Unifies the Viral Universe. *Annu. Rev. Biochem.* **2012**, *81*, 795–822, doi:10.1146/annurev-biochem-060910-095130.
9. Koonin, E. V.; Dolja, V. V.; Krupovic, M.; Varsani, A.; Wolf, Y.I.; Yutin, N.; Zerbini, F.M.; Kuhn, J.H. Global Organization and Proposed Megataxonomy of the Virus World. *Microbiol. Mol. Biol. Rev.* **2020**, *84*, doi:10.1128/mmbr.00061-19.
10. Liu, Y.; Demina, T.A.; Roux, S.; Aiewsakun, P.; Kazlauskas, D.; Simmonds, P.; Prangishvili, D.; Oksanen, H.M.; Krupovic, M. Diversity, Taxonomy, and Evolution of Archaeal Viruses of the Class Caudoviricetes. *PLoS Biol.* **2021**, *19*, 1–22, doi:10.1371/journal.pbio.3001442.
11. Oren, A. Taxonomy of Halophilic Archaea: Current Status and Future Challenges. *Extremophiles* 2014, *18*, 825–834.
12. Atanasova, N.S.; Bamford, D.H.; Oksanen, H.M. Haloarchaeal Virus Morphotypes. *Biochimie* **2015**, *118*, 333–343, doi:10.1016/j.biochi.2015.07.002.
13. Demina, T.A.; Pietilä, M.K.; Svirskaitė, J.; Ravantti, J.J.; Atanasova, N.S.; Bamford, D.H.; Oksanen, H.M. HCIV-1 and Other Tailless Icosahedral Internal Membrane-Containing Viruses of the Family Sphaerolipoviridae. *Viruses* **2017**, *9*, doi:10.3390/v9020032.
14. Demina, T.A.; Oksanen, H.M. Pleomorphic Archaeal Viruses: The Family Pleolipoviridae Is Expanding by Seven New Species. *Arch. Virol.* **2020**, *165*, 2723–2731, doi:10.1007/s00705-020-04689-1.

15. Bath, C.; Dyall-Smith, M.L. His1, an Archaeal Virus of TheFuselloviridae Family That Infects Haloarcula Hispanica. *J. Virol.* **1998**, *72*, 9392–9395, doi:10.1128/jvi.72.11.9392-9395.1998.

16. Senciļo, A.; Jacobs-Sera, D.; Russell, D.A.; Ko, C.C.; Bowman, C.A.; Atanasova, N.S.; Oštrlund, E.; Oksanen, H.M.; Bamford, D.H.; Hatfull, G.F.; et al. Snapshot of Haloarchaeal Tailed Virus Genomes. *RNA Biol.* **2013**, *10*, 803–816, doi:10.4161/rna.24045.

17. Trojet, S.N.; Caumont-Sarcos, A.; Perrody, E.; Comeau, A.M.; Krisch, H.M. The Gp38 Adhesins of the T4 Superfamily: A Complex Modular Determinant of the Phage's Host Specificity. *Genome Biol. Evol.* **2011**, *3*, 674–686, doi:10.1093/gbe/evr059.

18. Dunne, M.; Denyes, J.M.; Arndt, H.; Loessner, M.J.; Leiman, P.G.; Klumpp, J. Salmonella Phage S16 Tail Fiber Adhesin Features a Rare Polyglycine Rich Domain for Host Recognition. *Structure* **2018**, *26*, 1573-1582.e4, doi:10.1016/j.str.2018.07.017.

19. Atanasova, N.S.; Demina, T.A.; Buivydas, A.; Bamford, D.H.; Oksanen, H.M. Archaeal Viruses Multiply: Temporal Screening in a Solar Saltern. *Viruses* **2015**, *7*, 1902–1926, doi:10.3390/v7041902.

20. Li, Y.; Pan, S.; Zhang, Y.; Ren, M.; Feng, M.; Peng, N.; Chen, L.; Liang, Y.X.; She, Q. Harnessing Type i and Type III CRISPR-Cas Systems for Genome Editing. *Nucleic Acids Res.* **2015**, *44*, doi:10.1093/nar/gkv1044.

21. Albers, S.V.; Driessen, A.J.M. Conditions for Gene Disruption by Homologous Recombination of Exogenous DNA into the Sulfolobus Solfataricus Genome. *Archaea* **2008**, *2*, 145–149, doi:10.1155/2008/948014.

22. Lewis, A.M.; Recalde, A.; Bräsen, C.; Counts, J.A.; Nussbaum, P.; Bost, J.; Schocke, L.; Shen, L.; Willard, D.J.; Quax, T.E.F.; et al. The Biology of Thermoacidophilic Archaea from the Order Sulfolobales. *FEMS Microbiol. Rev.* 2021, *45*.

23. Leigh, J.A.; Albers, S.-V.V.; Atomi, H.; Allers, T. Model Organisms for Genetics in the Domain Archaea: Methanogens, Halophiles, Thermococcales and Sulfolobales. *FEMS Microbiol. Rev.* **2011**, *35*, 577–608, doi:10.1111/j.1574-6976.2011.00265.x.

24. Wagner, M.; van Wolferen, M.; Wagner, A.; Lassak, K.; Meyer, B.H.; Reimann, J.; Albers, S.V. Versatile Genetic Tool Box for the Crenarchaeote Sulfolobus Acidocaldarius. *Front. Microbiol.* **2012**, *3*, 1–12, doi:10.3389/fmicb.2012.00214.

25. Iverson, E.; Stedman, K. A Genetic Study of SSV1, the Prototypical Fusellovirus. *Front. Microbiol.* **2012**, *3*, 1–7, doi:10.3389/fmicb.2012.00200.

26. Wiedenheft, B.; Stedman, K.; Roberto, F.; Willits, D.; Gleske, A.-K.; Zoeller, L.; Snyder, J.; Douglas, T.; Young, M. Comparative Genomic Analysis of Hyperthermophilic Archaeal Fuselloviridae Viruses . *J. Virol.* **2004**, *78*, 1954–1961, doi:10.1128/jvi.78.4.1954-1961.2004.

27. Fulton, J.; Bothner, B.; Lawrence, M.; Johnson, J.E.; Douglas, T.; Young, M. Genetics, Biochemistry and Structure of the Archaeal Virus STIV. *Biochem. Soc. Trans.* **2009**, *37*, 114–117, doi:10.1042/BST0370114.

28. Xiang, X.; Chen, L.; Huang, X.; Luo, Y.; She, Q.; Huang, L. Sulfolobus Tengchongensis Spindle-Shaped Virus STSV1: Virus-Host Interactions and Genomic Features . *J. Virol.* **2005**, *79*, 8677–8686, doi:10.1128/jvi.79.14.8677-8686.2005.
29. Atanasova, N.S.; Roine, E.; Oren, A.; Bamford, D.H.; Oksanen, H.M. Global Network of Specific Virus-Host Interactions in Hypersaline Environments. *Environ. Microbiol.* **2012**, *14*, 426–440, doi:10.1111/j.1462-2920.2011.02603.x.
30. Svirskaitė, J.; Oksanen, H.M.; Daugelavičius, R.; Bamford, D.H. Monitoring Physiological Changes in Haloarchaeal Cell during Virus Release. *Viruses* **2016**, *8*, doi:10.3390/v8030059.
31. Santos-Pérez, I.; Charro, D.; Gil-Carton, D.; Azkargorta, M.; Elortza, F.; Bamford, D.H.; Oksanen, H.M.; Abrescia, N.G.A. Structural Basis for Assembly of Vertical Single β-Barrel Viruses. *Nat. Commun.* **2019**, *10*, 1184, doi:10.1038/s41467-019-08927-2.
32. Pietilä, M.K.; Atanasova, N.S.; Manole, V.; Liljeroos, L.; Butcher, S.J.; Oksanen, H.M.; Bamford, D.H. Virion Architecture Unifies Globally Distributed Pleolipoviruses Infecting Halophilic Archaea. *J. Virol.* **2012**, *86*, 5067–5079, doi:10.1128/JVI.06915-11.
33. El Omari, K.; Li, S.; Kotecha, A.; Walter, T.S.; Bignon, E.A.; Harlos, K.; Somerharju, P.; De Haas, F.; Clare, D.K.; Molin, M.; et al. The Structure of a Prokaryotic Viral Envelope Protein Expands the Landscape of Membrane Fusion Proteins. *Nat. Commun.* **2019**, *10*, doi:10.1038/s41467-019-08728-7.
34. Pietilä, M.K.; Atanasova, N.S.; Oksanen, H.M.; Bamford, D.H. Modified Coat Protein Forms the Flexible Spindle-Shaped Virion of Haloarchaeal Virus His1. *Environ. Microbiol.* **2013**, *15*, 1674–1686, doi:10.1111/1462-2920.12030.
35. Pohlschroder, M.; Schulze, S. Haloferax Volcanii. *Trends Microbiol.* 2019, *27*, 86–87.
36. Hartman, A.L.; Norais, C.; Badger, J.H.; Delmas, S.; Haldenby, S.; Madupu, R.; Robinson, J.; Khouri, H.; Ren, Q.; Lowe, T.M.; et al. The Complete Genome Sequence of Haloferax Volcanii DS2, a Model Archaeon. *PLoS One* **2010**, *5*, doi:10.1371/journal.pone.0009605.
37. Allers, T.; Ngo, H.P.; Mevarech, M.; Lloyd, R.G. Development of Additional Selectable Markers for the Halophilic Archaeon Haloferax Volcanii Based on the LeuB and TrpA Genes. *Appl. Environ. Microbiol.* **2004**, *70*, 943–953, doi:10.1128/AEM.70.2.943-953.2004.
38. Strillinger, E.; Grötzinger, S.W.; Allers, T.; Eppinger, J.; Weuster-Botz, D. Production of Halophilic Proteins Using Haloferax Volcanii H1895 in a Stirred-Tank Bioreactor. *Appl. Microbiol. Biotechnol.* **2016**, *100*, 1183–1195, doi:10.1007/s00253-015-7007-1.
39. Stachler, A.-E. Das CRISPR-Cas-System von Haloferax Volcanii: CRISPRi Und Autoimmunität. **2017**.
40. Bisson-Filho, A.W.; Zheng, J.; Garner, E. Archaeal Imaging: Leading the Hunt for New Discoveries. *Mol. Biol. Cell* 2018, *29*, 1675–1681.

41. Walsh, J.C.; Angstmann, C.N.; Bisson-Filho, A.W.; Garner, E.C.; Duggin, I.G.; Curmi, P.M.G. Division Plane Placement in Pleomorphic Archaea Is Dynamically Coupled to Cell Shape. *Mol. Microbiol.* **2019**, *112*, 785–799, doi:10.1111/mmi.14316.

42. Duggin, I.G.; Aylett, C.H.S.; Walsh, J.C.; Michie, K.A.; Wang, Q.; Turnbull, L.; Dawson, E.M.; Harry, E.J.; Whitchurch, C.B.; Amos, L.A.; et al. CetZ Tubulin-like Proteins Control Archaeal Cell Shape. *Nature* **2015**, *519*, 362–365, doi:10.1038/nature13983.

43. Hawkins, M.; Malla, S.; Blythe, M.J.; Nieduszynski, C.A.; Allers, T. Accelerated Growth in the Absence of DNA Replication Origins. *Nature* **2013**, *503*, 544–547, doi:10.1038/nature12650.

44. Haque, R.U.; Paradisi, F.; Allers, T. Haloferax Volcanii for Biotechnology Applications: Challenges, Current State and Perspectives. *Appl. Microbiol. Biotechnol.* 2020, *104*, 1371–1382.

45. Abdul-Halim, M.F.; Schulze, S.; DiLucido, A.; Pfeiffer, F.; Filho, A.W.B.; Pohlschroder, M. Lipid Anchoring of Archaeosortase Substrates and Midcell Growth in Haloarchaea. *MBio* **2020**, *11*, doi:10.1128/mBio.00349-20.

46. Li, Z.; Kinosita, Y.; Rodriguez-Franco, M.; Nußbaum, P.; Braun, F.; Delpech, F.; Quax, T.E.F.; Albers, S.V. Positioning of the Motility Machinery in Halophilic Archaea. *MBio* **2019**, *10*, doi:10.1128/mBio.00377-19.

47. Nußbaum, P.; Ithurbide, S.; Walsh, J.C.; Patro, M.; Delpech, F.; Rodriguez-Franco, M.; Curmi, P.M.G.; Duggin, I.G.; Quax, T.E.F.; Albers, S.-V.V. An Oscillating MinD Protein Determines the Cellular Positioning of the Motility Machinery in Archaea. *Curr. Biol.* **2020**, *30*, 4956-4972.e4, doi:10.1016/j.cub.2020.09.073.

48. Jarrell, K.F.; Ding, Y.; Meyer, B.H.; Albers, S.-V.; Kaminski, L.; Eichler, J. N-Linked Glycosylation in Archaea: A Structural, Functional, and Genetic Analysis. *Microbiol. Mol. Biol. Rev.* **2014**, *78*, 304–341, doi:10.1128/mmbr.00052-13.

49. de Silva, R.T.; Abdul-Halim, M.F.; Pittrich, D.A.; Pohlschroder, M.; Duggin, I.G.; Brown, H.J.; Pohlschroder, M.; Duggin, I.G. Improved Growth and Morphological Plasticity of Haloferax Volcanii. *Microbiol. (United Kingdom)* **2021**, *167*, 2020.05.04.078048, doi:10.1099/mic.0.001012.

50. Kinosita, Y.; Mikami, N.; Li, Z.; Braun, F.; Quax, T.E.F.; van der Does, C.; Ishmukhametov, R.; Albers, S.V.; Berry, R.M. Motile Ghosts of the Halophilic Archaeon, Haloferax Volcanii. *Proc. Natl. Acad. Sci. U. S. A.* **2020**, *117*, 26766–26772, doi:10.1073/pnas.2009814117.

51. Li, Z.; Rodriguez-Franco, M.; Albers, S.V.; Quax, T.E.F. The Switch Complex ArlCDE Connects the Chemotaxis System and the Archaellum. *Mol. Microbiol.* **2020**, doi:10.1111/mmi.14527.

52. Quax, T.E.F.; Altegoer, F.; Rossi, F.; Li, Z.; Rodriguez-Franco, M.; Kraus, F.; Bange, G.; Albers, S.V. Structure and Function of the Archaeal Response Regulator CheY. *Proc. Natl. Acad. Sci. U. S. A.* **2018**, *115*, E1259–E1268, doi:10.1073/pnas.1716661115.

53. Esquivel, R.N.; Schulze, S.; Xu, R.; Hippler, M.; Pohlschroder, M. Identification of *Haloferax Volcanii* Pilin *N* -Glycans with Diverse Roles in Pilus Biosynthesis, Adhesion, and Microcolony Formation. *J. Biol. Chem.* **2016**, *291*, 10602–10614, doi:10.1074/jbc.M115.693556.
54. Esquivel, R.N.; Xu, R.; Pohlschroder, M. Novel Archaeal Adhesion Pilins with a Conserved N Terminus. *J. Bacteriol.* **2013**, *195*, 3808–3818, doi:10.1128/JB.00572-13.
55. Maier, L.K.; Marchfelder, A. It's All about the T: Transcription Termination in Archaea. *Biochem. Soc. Trans.* 2019, *47*, 461–468.
56. Humbard, M.A.; Miranda, H. V.; Lim, J.M.; Krause, D.J.; Pritz, J.R.; Zhou, G.; Chen, S.; Wells, L.; Maupin-Furlow, J.A. Ubiquitin-like Small Archaeal Modifier Proteins (SAMPs) in Haloferax Volcanii. *Nature* **2010**, *463*, 54–60, doi:10.1038/nature08659.
57. Li, M.; Liu, H.; Han, J.; Liu, J.; Wang, R.; Zhao, D.; Zhou, J.; Xiang, H. Characterization of CRISPR RNA Biogenesis and Cas6 Cleavage-Mediated Inhibition of a Provirus in the Haloarchaeon Haloferax Mediterranei. *J. Bacteriol.* **2013**, *195*, 867–875, doi:10.1128/JB.01688-12.
58. Nuttall, S.D.; Smith, M.L.D. HF1 and HF2: Novel Bacteriophages of Halophilic Archaea. *Virology* **1993**, *197*, 678–684, doi:10.1006/viro.1993.1643.
59. Mizuno, C.M.; Prajapati, B.; Lucas-Staat, S.; Sime-Ngando, T.; Forterre, P.; Bamford, D.H.; Prangishvili, D.; Krupovic, M.; Oksanen, H.M. Novel Haloarchaeal Viruses from Lake Retba Infecting Haloferax and Halorubrum Species. *Environ. Microbiol.* **2019**, *21*, 2129–2147, doi:10.1111/1462-2920.14604.
60. Tittes, C.; Schwarzer, S.; Pfeiffer, F.; Dyall-Smith, M.; Rodriguez-Franco, M.; Oksanen, H.M.; Quax, T.E.F.F. Cellular and Genomic Properties of Haloferax Gibbonsii LR2-5, the Host of Euryarchaeal Virus HFTV1. *Front. Microbiol.* **2021**, *12*, 1–14, doi:10.3389/fmicb.2021.625599.
61. Dyall-Smith, M. The Halohandbook: Protocols for Halobacterial Genetics. *Mark Dyall-Smith, Martinsried, Ger.* **2008**, 1–144.
62. Guindon, S.; Dufayard, J.F.; Lefort, V.; Anisimova, M.; Hordijk, W.; Gascuel, O. New Algorithms and Methods to Estimate Maximum-Likelihood Phylogenies: Assessing the Performance of PhyML 3.0. *Syst. Biol.* **2010**, *59*, 307–321, doi:10.1093/sysbio/syq010.
63. Yu, G.; Smith, D.K.; Zhu, H.; Guan, Y.; Lam, T.T. <scp>ggtree</Scp> : An <scp>r</Scp> Package for Visualization and Annotation of Phylogenetic Trees with Their Covariates and Other Associated Data. *Methods Ecol. Evol.* **2017**, *8*, 28–36, doi:10.1111/2041-210X.12628.
64. Moraru, C.; Varsani, A.; Kropinski, A.M. VIRIDIC—A Novel Tool to Calculate the Intergenomic Similarities of Prokaryote-Infecting Viruses. *Viruses* **2020**, *12*, doi:10.3390/v12111268.
65. Sullivan, M.J.; Petty, N.K.; Beatson, S.A. Easyfig: A Genome Comparison Visualizer. *Bioinformatics* **2011**, *27*, 1009–1010, doi:10.1093/bioinformatics/btr039.
66. Katoh, K.; Standley, D.M. MAFFT Multiple Sequence Alignment Software Version 7: Improvements in Performance and Usability. *Mol. Biol. Evol.* **2013**, *30*, 772–780, doi:10.1093/molbev/mst010.

67. Nguyen, L.T.; Schmidt, H.A.; Von Haeseler, A.; Minh, B.Q. IQ-TREE: A Fast and Effective Stochastic Algorithm for Estimating Maximum-Likelihood Phylogenies. *Mol. Biol. Evol.* **2015**, *32*, 268–274, doi:10.1093/molbev/msu300.

68. Kalyaanamoorthy, S.; Minh, B.Q.; Wong, T.K.F.; Von Haeseler, A.; Jermiin, L.S. ModelFinder: Fast Model Selection for Accurate Phylogenetic Estimates. *Nat. Methods* **2017**, *14*, 587–589, doi:10.1038/nmeth.4285.

69. Suchard, M.A.; Lemey, P.; Baele, G.; Ayres, D.L.; Drummond, A.J.; Rambaut, A. Bayesian Phylogenetic and Phylodynamic Data Integration Using BEAST 1.10. *Virus Evol.* **2018**, *4*, doi:10.1093/ve/vey016.

70. Whelan, S.; Goldman, N. A General Empirical Model of Protein Evolution Derived from Multiple Protein Families Using a Maximum-Likelihood Approach. *Mol. Biol. Evol.* **2001**, *18*, 691–699, doi:10.1093/oxfordjournals.molbev.a003851.

71. Henikoff, S.; Henikoff, J.G. Amino Acid Substitution Matrices from Protein Blocks. *Proc. Natl. Acad. Sci. U. S. A.* **1992**, *89*, 10915–10919, doi:10.1073/pnas.89.22.10915.

72. Kingman, J.F.C. The Coalescent. *Stoch. Process. their Appl.* **1982**, *13*, 235–248, doi:10.1016/0304-4149(82)90011-4.

73. Lemey, P.; Rambaut, A.; Drummond, A.J.; Suchard, M.A. Bayesian Phylogeography Finds Its Roots. *PLoS Comput. Biol.* **2009**, *5*, doi:10.1371/journal.pcbi.1000520.

74. Minin, V.N.; Suchard, M.A. Counting Labeled Transitions in Continuous-Time Markov Models of Evolution. *J. Math. Biol.* **2008**, *56*, 391–412, doi:10.1007/s00285-007-0120-8.

75. Rambaut, A.; Drummond, A.J.; Xie, D.; Baele, G.; Suchard, M.A. Posterior Summarization in Bayesian Phylogenetics Using Tracer 1.7. *Syst. Biol.* **2018**, *67*, 901–904, doi:10.1093/sysbio/syy032.

76. Rodriguez-Valera, F.; Juez, G.; Kushner, D.J. Halobacterium Mediterranei Spec, Nov., a New Carbohydrate-Utilizing Extreme Halophile. *Syst. Appl. Microbiol.* **1983**, *4*, 369–381, doi:10.1016/S0723-2020(83)80021-6.

77. Kumar, V.; Singh, B.; van Belkum, M.J.; Diep, D.B.; Chikindas, M.L.; Ermakov, A.M.; Tiwari, S.K. Halocins, Natural Antimicrobials of Archaea: Exotic or Special or Both? *Biotechnol. Adv.* 2021, *53*.

78. Atanasova, N.S.; Pietilä, M.K.; Oksanen, H.M. Diverse Antimicrobial Interactions of Halophilic Archaea and Bacteria Extend over Geographical Distances and Cross the Domain Barrier. *Microbiologyopen* **2013**, *2*, 811–825, doi:10.1002/mbo3.115.

79. Dyall-Smith, M.; Tang, S.L.; Russ, B.; Chiang, P.W.; Pfeiffer, F. Comparative Genomics of Two New HF1-like Haloviruses. *Genes (Basel).* **2020**, *11*, doi:10.3390/genes11040405.

80. Cerritelli, M.E.; Wall, J.S.; Simon, M.N.; Conway, J.F.; Steven, A.C. Stoichiometry and Domainal Organization of the Long Tail-Fiber of Bacteriophage T4: A Hinged Viral Adhesin. *J. Mol. Biol.* **1996**, *260*, 767–780, doi:10.1006/jmbi.1996.0436.

81. Gambelli, L.; Meyer, B.H.; McLaren, M.; Sanders, K.; Quax, T.E.F.; Gold, V.A.M.; Albers, S.V.; Daum, B. Architecture and Modular Assembly of Sulfolobus S-Layers Revealed by Electron Cryotomography. *Proc. Natl. Acad. Sci. U. S. A.* **2019**, *116*, 25278–25286, doi:10.1073/pnas.1911262116.

82. Zink, I.A.; Pfeifer, K.; Wimmer, E.; Sleytr, U.B.; Schuster, B.; Schleper, C. CRISPR-Mediated Gene Silencing Reveals Involvement of the Archaeal S-Layer in Cell Division and Virus Infection. *Nat. Commun.* **2019**, *10*, doi:10.1038/s41467-019-12745-x.

Supplementary Material

Supplementary Table S1. ***Haloferax*** **strains used in the study**

Strain	Reference
Haloferax volcanii H26	[1]
Haloferax sp. s5a-1	[2]
Haloferax sp. SP10-1	[2]
Haloferax sp. SS9-6	[3]
Haloferax sp. SS10-6	[3]
Haloferax sp. SS10-7	[3]
Haloferax sp. LR1-5	[4]
Haloferax sp. LR1-14	[4]
Haloferax sp. LR1-18	[4]
Haloferax sp. LR1-19	[4]
Haloferax sp. LR1-24	[4]
Haloferax gibbonsii LR2-5	[4,5]
Haloferax sp. LR2-16	[4]
Haloferax mediterranei DSM 1411	[6]

Supplementary Table S2. Viruses used in the study

Virus name	Virus abbreviation	Virus origin	Morphotype	Genome length (bp, nt)	Genome Acc. No.	Reference for virus	*Genus*	*Family*	*Isolation host*	*Host used in this study*	Reference for host used
Halorubrum head-tail virus 8	HRTV-8	solar saltern, Samut Sakhon, Thailand	myovirus	74519	KC292020	PMID: 23470522	*Haloferacalesvirus*	*Hafunaviridae*	*Halorubrum* sp. B2-2	*Halorubrum* sp. B2-2	PMID: 22003883
Halorubrum tailed virus 14	HRTV-14	solar saltern, Samut Sakhon, Thailand	myovirus	74355	MZ334492	PMID: 25866903	*Haloferacalesvirus*	*Hafunaviridae*	*Halorubrum* sp. SS6-2	*Halorubrum* sp. SS10-9	PMID: 25866903
Halorubrum tailed virus 17	HRTV-17	solar saltern, Samut Sakhon, Thailand	myovirus	74754	MZ334493	PMID: 25866903	*Haloferacalesvirus*	*Hafunaviridae*	*Halorubrum* sp. SS9-12	*Halobacterium* sp. SS6-4	PMID: 25866903
Halorubrum tailed virus 19	HRTV-19	solar saltern, Samut Sakhon, Thailand	myovirus	77739	MZ334494	PMID: 25866903	*Haloferacalesvirus*	*Hafunaviridae*	*Halorubrum* sp. SS10-3	*Halorubrum* sp. SS10-3	PMID: 25866903
Halorubrum tailed virus 23	HRTV-23	solar saltern, Samut Sakhon, Thailand	myovirus	77739	MZ334495	PMID: 25866903	*Haloferacalesvirus*	*Hafunaviridae*	*Halorubrum* sp. SS10-9	*Halorubrum* sp. SS10-9	PMID: 25866903
Halorubrum head-tail virus 10	HRTV-10	solar saltern, Eilat, Israel	myovirus	76759	MZ334496	PMID: 22003883	*Haloferacalesvirus*	*Hafunaviridae*	*Halorubrum* sp. B2-2	*Halorubrum* sp. B2-2	PMID: 22003883
Halorubrum tailed virus 18	HRTV-18	solar saltern, Samut Sakhon, Thailand	myovirus	76361	MZ334497	PMID: 25866903	*Haloferacalesvirus*	*Hafunaviridae*	*Halorubrum* sp. SS10-3	*Halorubrum* sp. SS10-3	PMID: 25866903
Halorubrum tailed virus 20	HRTV-20	solar saltern, Samut Sakhon, Thailand	myovirus	76259	MZ334498	PMID: 25866903	*Haloferacalesvirus*	*Hafunaviridae*	*Halorubrum* sp. SS10-9	*Halorubrum* sp. SS10-9	PMID: 25866903
Halorubrum tailed virus 22	HRTV-22	solar saltern, Samut Sakhon, Thailand	myovirus	76812	MZ334499	PMID: 25866903	*Haloferacalesvirus*	*Hafunaviridae*	*Halorubrum* sp. SS10-9	*Halorubrum* sp. SS10-9	PMID: 25866903
Halorubrum tailed virus 26	HRTV-26	solar saltern, Samut Sakhon, Thailand	myovirus	77578	MZ334500	PMID: 25866903	*Haloferacalesvirus*	*Hafunaviridae*	*Halorubrum* sp. SS13-13	*Halorubrum* sp. SS10-9	PMID: 25866903
Halorubrum sodomense tailed virus 4	HSTV-4	solar saltern, Samut Sakhon, Thailand	myovirus	75181	MZ334501	PMID: 25866903	*Haloferacalesvirus*	*Hafunaviridae*	*Halorubrum sodomense*	*Halorubrum* sp. SP3-3	PMID: 22003883
Halorubrum head-tail virus 5	HRTV-5	solar saltern, Margherita di Savoia, Italy	myovirus	76134	KC292022	PMID: 23470522	*Haloferacalesvirus*	*Hafunaviridae*	*Halorubrum* sp. s5a-3	*Halorubrum* sp. s5a-3	PMID: 22003883
Haloarcula californiae tailed virus 7	HCTV-7 (1)	solar saltern, Samut Sakhon, Thailand	myovirus	76008	MZ334502	PMID: 25866903	*Haloferacalesvirus*	*Hafunaviridae*	*Haloarcula californiae*	*Haloarcula californiae*	PMID: 6286602
Haloarcula californiae tailed virus 12	HCTV-12 (1)	solar saltern, Samut Sakhon, Thailand	myovirus	76008	MZ334502	PMID: 25866904	*Haloferacalesvirus*	*Hafunaviridae*	*Haloarcula californiae*	*Haloarcula californiae*	PMID: 6286602
Haloarcula californiae tailed virus 9	HCTV-9	solar saltern, Samut Sakhon, Thailand	myovirus	76008	MZ334503	PMID: 25866903	*Haloferacalesvirus*	*Hafunaviridae*	*Haloarcula californiae*	*Halorubrum* sp. SS8-2	PMID: 25866903
Haloarcula californiae tailed virus 11	HCTV-11	solar saltern, Samut Sakhon, Thailand	myovirus	76008	MZ334504	PMID: 25866903	*Haloferacalesvirus*	*Hafunaviridae*	*Haloarcula californiae*	*Haloarcula californiae*	PMID: 6286602
Halorubrum head-tail virus 9	HRTV-9	solar saltern, Eilat, Israel	myovirus	75429	MZ334505	PMID: 22003883	*Haloferacalesvirus*	*Hafunaviridae*	*Halorubrum* sp. B2-2	*Halorubrum* sp. B2-2	PMID: 22003883
Halorubrum tailed virus 16	HRTV-16	solar saltern, Samut Sakhon, Thailand	myovirus	77109	MZ334506	PMID: 25866903	*Haloferacalesvirus*	*Hafunaviridae*	*Halorubrum* sp. SS6-2	*Haloterrigena* sp. SS13-7	PMID: 25866903

Haloferax strains used to detect growth inhibition zones (potential halocins)																												
H26		**s5a-1**		**SP10-1**		**SS9-6**		**SS10-6**		**SS10-7**		**LR1-5**		**LR1-14**		**LR1-18**		**LR1-19**		**LR1-24**		**LR2-5**		**LR2-16**		***H.mediterranei***	
10^0	10^-2	10^0	10^-2	10^0	10^-2	10^0	10^-2	10^0	10^-2	10^0	10^-2	10^0	10^-2	10^0	10^-2	10^0	10^-2	10^0	10^-2	10^0	10^-2	10^0	10^-2	10^0	10^-2	10^0	10^-2
-	-	-	-	-	-	+	+	-	-	+	+	-	-	+	-	-	-	-	-	+	-	-	-	+	-	+	+
-	-	-	-	-	-	-	-	-	-	-	-	-	-	+	-	-	-	+	-	+	-	-	-	+	-	+	+
-	-	-	-	-	-	-	-	-	-	-	-		-	-	-	-	-	-	-	-	-	+	-	-	-	-	-
-	-	-	-	-	-	+	+	-	-	+	+	-	-	+	-	-	-	-	-	+	-	+	-	-	-	+	+
-	-	+	-	-	-	+	+	+	+	+	+	-	-	+	-	-	-	-	-	+	-	-	-	+	-	+	+
-	-	-	-	-	-	-	-	-	-	-	-	-	-	+	-	+	-	+	+	+	-	+	+	+	-	-	-
-	-	-	-	-	-	-	-	-	-	-	-	-	-	+	-	-	-	+	-	+	-	+	+	+	-	-	-
-	-	+	-	-	-	+	-	-	-	-	-	-	-	+	-	+	+	+	+	+	-	+	+	+	-	-	-
-	-	-	-	-	-	+	-	+	-	+	+	-	-	+	-	+	-	-	-	+	-	-	-	+	-	+	+
-	-	-	-	-	-	-	-	-	-	-	-	-	-	+	-	+	+	+	+	+	-	+	+	+	-	-	-
-	-	-	-	-	-	-	-	-	-	-	-	-	-	-	-	-	-	-	-	-	-	-	-	-	-	-	-
-	-	-	-	-	-	-	-	-	-	-	-	-	-	+	-	-	-	+	-	+	-	-	-	+	-	-	-
-	-	-	-	+	+	-	-	-	-	-	-	-	-	+	-	-	-	+	-	+	-	-	-	+	-	-	-
-	-	-	-	+	+	-	-	-	-	-	-	-	-	+	-	-	-	+	-	+	-	+	-	+	-	-	-
+	+	-	-	+	+	+	-	-	-	-	-	-	-	+	-	+	+	-	-	+	-	-	-	+	-	-	-
+	+	-	-	+	-	-	-	-	-	-	-	-	-	+	-	+	+	-	-	+	-	-	-	+	-	-	-
-	-	-	-	-	-	-	-	-	-	-	-	-	-	-	-	+	-	-	-	-	-	-	-	-	-	-	-
-	-	-	-	-	-	-	-	-	-	-	-	-	-	-	-	-	-	-	-	+	-	+	-	-	-	-	-

Virus name	Virus abbreviation	Virus origin	Morphotype	Genome length (bp, nt)	Genome Acc. No.	Reference for virus	*Genus*	*Family*	*Isolation host*	*Host used in this study*	Reference for host used
Haloarcula californiae tailed virus 8	HCTV-8	solar saltern, Samut Sakhon, Thailand	myovirus	75019	MZ334507	PMID: 25866903	*Haloferacalesvirus*	*Hafunaviridae*	*Haloarcula californiae*	*Haloarcula californiae*	PMID: 6286602
Haloarcula californiae tailed virus 10	HCTV-10	solar saltern, Samut Sakhon, Thailand	myovirus	75019	MZ334508	PMID: 25866903	*Haloferacalesvirus*	*Hafunaviridae*	*Haloarcula californiae*	*Halorubrum sodomense*	doi.org/10.1099/00207713-33-2-381
Haloarcula japonica head-tail virus 1	HJTV-1	solar saltern, Margherita di Savoia, Italy	myovirus	78012	MZ334509	PMID: 22003883	*Haloferacalesvirus*	*Hafunaviridae*	*Haloarcula japonica*	*Haloarcula japonica*	doi.org/10.1016/S0723-2020(11)80165-7
Halorubrum tailed virus 13	HRTV-13	solar saltern, Samut Sakhon, Thailand	myovirus	76666	MZ334510	PMID: 25866903	*Haloferacalesvirus*	*Hafunaviridae*	*Halorubrum* sp. SS8-2	*Halorubrum* sp. SS8-2	PMID: 25866903
Halorubrum tailed virus 21	HRTV-21	solar saltern, Samut Sakhon, Thailand	myovirus	76556	MZ334511	PMID: 25866903	*Haloferacalesvirus*	*Hafunaviridae*	*Halorubrum* sp. SS10-9	*Halorubrum* sp. SS10-9	PMID: 25866903
Halorubrum tailed virus 24	HRTV-24	solar saltern, Samut Sakhon, Thailand	myovirus	77537	MZ334512	PMID: 25866903	*Haloferacalesvirus*	*Hafunaviridae*	*Halorubrum* sp. SS10-9	*Halorubrum* sp. SS10-9	PMID: 25866903
Haloarcula japonica head-tail virus 2	HJTV-2	solar saltern, Samut Sakhon, Thailand	myovirus	76821	MZ334513	PMID: 22003883	*Haloferacalesvirus*	*Hafunaviridae*	*Haloarcula japonica*	*Haloarcula japonica*	doi.org/10.1016/S0723-2020(11)80165-7
Halorubrum sodomense head-tail virus 3	HSTV-3	solar saltern, Eilat, Israel	myovirus	76908	MZ334514	PMID: 22003883	*Haloferacalesvirus*	*Hafunaviridae*	*Halorubrum sodomense*	*Halorubrum sodomense*	doi.org/10.1099/00207713-33-2-381
Haloarcula japonica tailed virus 3	HJTV-3	solar saltern, Samut Sakhon, Thailand	myovirus	77353	MZ334515	PMID: 25866903	*Haloferacalesvirus*	*Hafunaviridae*	*Haloarcula japonica*	*Haloarcula japonica*	doi.org/10.1016/S0723-2020(11)80165-7
Halorubrum tailed virus 15	HRTV-15	solar saltern, Samut Sakhon, Thailand	myovirus	76242	MZ334516	PMID: 25866903	*Haloferacalesvirus*	*Hafunaviridae*	*Halorubrum* sp. SS6-2	*Halorubrum* sp. SS6-2	PMID: 25866903
Halorubrum sodomense head-tail virus 2	HSTV-2	solar saltern, Eilat, Israel	myovirus	68527	KC117376	PMID: 23283946	*Mincapvirus*	*Hafunaviridae*	*Halorubrum sodomense*	*Halorubrum sodomense*	doi.org/10.1099/00207713-33-2-381
Halorubrum head-tail virus 7	HRTV-7	solar saltern, Margherita di Savoia, Italy	myovirus	69048	KC292021	PMID: 23470522	*Mincapvirus*	*Hafunaviridae*	*Halorubrum* sp. B2-2	*Halorubrum* sp. B2-2	PMID: 22003883
Halorubrum head-tail virus 2	HRTV-2	solar saltern, Margherita di Savoia, Italy	myovirus	68923	MZ334517	PMID: 22003883	*Mincapvirus*	*Hafunaviridae*	*Halorubrum* sp. s1-2	*Halorubrum* sp. s1-2	PMID: 22003883
Halorubrum head-tail virus 11	HRTV-11	solar saltern, Sečovlje, Slovenia	myovirus	71449	MZ334518	PMID: 22003883	*Mincapvirus*	*Hafunaviridae*	*Halorubrum* sp. SL-5	*Halorubrum* sp. SL-5	PMID: 22003883
Haloarcula californiae tailed virus 6	HCTV-6 (2)	solar saltern, Samut Sakhon, Thailand	myovirus	71672	MZ334519	PMID: 25866903	*Mincapvirus*	*Hafunaviridae*	*Haloarcula californiae*	*Haloarcula californiae*	PMID: 6286602
Haloarcula californiae tailed virus 13	HCTV-13 (2)	solar saltern, Samut Sakhon, Thailand	myovirus	71672	MZ334519	PMID: 25866904	*Mincapvirus*	*Hafunaviridae*	*Haloarcula californiae*	*Haloarcula californiae*	PMID: 6286602
Haloarcula californiae tailed virus 15	HCTV-15	solar saltern, Samut Sakhon, Thailand	myovirus	71672	MZ334520	PMID: 25866903	*Mincapvirus*	*Hafunaviridae*	*Haloarcula californiae*	*Haloarcula californiae*	PMID: 6286602
Halorubrum tailed virus 25	HRTV-25	solar saltern, Samut Sakhon, Thailand	myovirus	61934	MZ334521	PMID: 25866903	*Laminvirus*	*Hafunaviridae*	*Halorubrum* sp. SS13-12	*Halorubrum* sp. SS13-12	PMID: 25866903
Halorubrum tailed virus 27	HRTV-27	solar saltern, Samut Sakhon, Thailand	myovirus	56593	MZ334522	PMID: 25866903	*Minorvirus*	*Hafunaviridae*	*Halorubrum* sp. SS13-13	*Halorubrum* sp. SS10-9	PMID: 25866903

Haloferax strains used to detect growth inhibition zones (potential halocins)

H26		s5a-1		SP10-1		SS9-6		SS10-6		SS10-7		LR1-5		LR1-14		LR1-18		LR1-19		LR1-24		LR2-5		LR2-16		*H.mediterranei*	
10^0	10^-2	10^0	10^-2	10^0	10^-2	10^0	10^-2	10^0	10^-2	10^0	10^-2	10^0	10^-2	10^0	10^-2	10^0	10^-2	10^0	10^-2	10^0	10^-2	10^0	10^-2	10^0	10^-2	10^0	10^-2
-	-	-	-	+	+	-	-	-	-	-	-	-	-	+	-	-	-	+	-	+	-	+	-	+	-	-	-
+	+	-	-	+	-	-	-	+	+	-	-	-	-	+	+	-	-	-	-	-	-	+	+	+	-	+	+
-	-	-	-	-	-	-	-	-	-	-	-	-	-	+	-	-	-	+	+	+	-	+	+	+	-	+	+
-	-	-	-	-	-	+	+	-	-	+	-	-	-	+	-	-	-	+	-	+	-	-	-	+	-	+	+
+	+	+	-	-	-	+	-	-	-	-	-	-	-	+	-	+	-	+	+	+	-	+	-	+	-	-	-
-	-	-	-	-	-	-	-	+	+	-	-	-	-	+	-	-	-	-	-	-	-	-	-	-	-	+	+
-	-	-	-	-	-	-	-	-	-	-	-	-	-	+	-	+	+	+	+	+	-	+	+	+	-	-	-
-	-	-	-	-	-	-	-	-	-	-	-	-	-	-	-	-	-	-	-	-	-	-	-	-	-	+	+
-	-	-	-	-	-	-	-	-	-	-	-	-	-	-	-	-	-	-	-	-	-	+	+	-	-	-	-
-	-	+	+	-	-	+	+	+	-	+	-	-	-	+	-	+	+	-	-	+	-	-	-	+	-	-	-
-	-	-	-	-	-	+	-	-	-	+	-	-	-	+	-	-	-	+	+	+	-	+	+	+	-	+	+
-	-	-	-	-	-	+	-	-	-	-	-	-	-	+	-	+	+	-	-	+	-	+	+	+	-	-	-
+	+	-	-	-	-	+	-	-	-	+	-	-	-	+	+	+	+	+	+	+	-	+	+	+	+	-	-
+	-	-	-	-	-	+	-	-	-	+	-	-	-	+	-	+	+	+	+	+	+	+	+	+	+	-	-
-	-	+	+	-	-	-	-	-	-	-	-	-	-	-	-	-	-	-	-	-	-	+	+	+	+	+	+
-	-	-	-	-	-	-	-	-	-	-	-	-	-	+	-	-	-	+	+	+	-	+	+	+	-	+	+
-	-	-	-	-	-	+	-	-	-	+	-	-	-	+	-	+	+	-	-	+	-	+	+	+	-	+	+
-	-	-	-	-	-	+	-	-	-	-	-	-	-	+	-	-	-	-	-	+	-	-	-	+	-	-	-
-	-	-	-	-	-	+	+	-	-	+	-	-	-	+	-	-	-	-	-	+	-	-	-	+	-	-	-

Virus name	Virus abbreviation	Virus origin	Morphotype	Genome length (bp, nt)	Genome Acc. No.	Reference for virus	*Genus*	*Family*	*Isolation host*	*Host used in this study*	Reference for host used
Haloarcula vallismortis head-tail virus 1	HVTV-1	solar saltern, Samut Sakhon, Thailand	siphovirus	102319	KC117377	PMID 23733949	*Tredecimvirus*	*Druskaviridae*	*Haloarcula vallismortis*	*Haloarcula vallismortis*	PMID: 667737
Haloarcula vallismortis head-tail virus 2	HVTV-2	solar saltern, Samut Sakhon, Thailand	siphovirus	102319	MZ334523	PMID: 22003883	*Tredecimvirus*	*Druskaviridae*	*Haloarcula vallismortis*	*Haloarcula vallismortis*	PMID: 667737
Haloarcula californiae head-tail virus 5	HCTV-5	solar saltern, Samut Sakhon, Thailand	siphovirus	102105	KC292027	PMID: 23470522	*Tredecimvirus*	*Druskaviridae*	*Haloarcula californiae*	*Haloarcula californiae*	PMID: 6286602
Haloarcula californiae head-tail virus 1	HCTV-1	solar saltern, Margherita di Savoia, Italy	siphovirus	103257	KC292029	PMID: 23470522	*Hacavirus*	*Druskaviridae*	*Haloarcula californiae*	*Haloarcula californiae*	PMID: 6286602
Haloarcula californiae tailed virus 16	HCTV-16	solar saltern, Samut Sakhon, Thailand	siphovirus	104681	MZ334524	PMID: 25866903	*Hacavirus*	*Druskaviridae*	*Haloarcula californiae*	*Haloarcula californiae*	PMID: 6286602
Haloarcula head-tail virus 2	HATV-2	solar saltern, Eilat, Israel	myovirus	63301	MZ334525	PMID: 22003883	*Eilatmyovirus*	*Soleiviridae*	*Haloarcula* sp. E301-5	*Haloarcula* sp. E301-5	PMID: 22003883
Halogranum head-tail virus 1	HGTV-1	solar saltern, Samut Sakhon, Thailand	myovirus	143855	KC292026	PMID: 23470522	*Hagravirus*	*Halomagnusviridae*	*Halogranum* sp. SS5-1	*Halogranum* sp. SS5-1	PMID: 23470522
Haloferax tailed virus 1	HFTV1	saline lake Retba, Cape Verde Peninsula, Senegal	siphovirus	38059	MG550112	PMID: 30920125	*Retbasiphovirus*	*Haloferuviridae*	*Haloferax gibbonsii* LR2-5	*Haloferax gibbonsii* LR2-5	PMID: 33664716
Halorubrum tailed virus 29	HRTV-29	solar saltern, Samut Sakhon, Thailand	siphovirus	36603	MZ334526	PMID: 25866903	*Dipdavirus*	*Haloferuviridae*	*Halorubrum* sp. SS7-4	*Halorubrum* sp. SS7-4	PMID: 22357279
Halorubrum head-tail virus 4	HRTV-4	solar saltern, Margherita di Savoia, Italy	siphovirus	35722	KC292023	PMID: 23470522	*Saldibavirus*	*Haloferuviridae*	*Halorubrum* sp. s5a-3	*Halorubrum* sp. s5a-3	PMID: 22003883
Haloarcula tailed virus 3	HATV-3	solar saltern, Samut Sakhon, Thailand	siphovirus	42293	MZ334527	PMID: 25866903	*Hatrivirus*	*Pyrstoviridae*	*Haloarcula* sp. SS8-5	*Haloarcula* sp. SS8-5	PMID: 25866903
Haloarcula sinaiiensis head-tail virus 1	HSTV-1	solar saltern, Margherita di Savoia, Italy	podovirus	32189	KC117378	PMID: 23733949	*Lonfivirus*	*Shortaselviridae*	*Haloarcula sinaiiensis*	*Haloarcula sinaiiensis*	PMID: 6286602
Halorubrum tailed virus 28	HRTV-28	solar saltern, Samut Sakhon, Thailand	siphovirus	35270	MZ334528	PMID: 25866903	*Pormufvirus*	*Suolaviridae*	*Halorubrum* sp. SS8-7	*Halorubrum* sp. SS8-7	PMID: 25866903
Haloarcula californiae head-tail virus 2	HCTV-2	solar saltern, Samut Sakhon, Thailand	siphovirus	54291	KC292028	PMID: 23470522	*Samsavirus*	*Saparoviridae*	*Haloarcula californiae*	*Haloarcula californiae*	PMID: 6286602
Haloarcula hispanica head-tail virus 2	HHTV-2	solar saltern, Samut Sakhon, Thailand	siphovirus	52643	KC292024	PMID: 23470522	*Halohivirus*	*Saparoviridae*	*Haloarcula hispanica*	*Haloarcula hispanica*	doi.org/10.1016/S0723-2020(86)80152-7
Haloarcula hispanica head-tail virus 1	HHTV-1	solar saltern, Margherita di Savoia, Italy	siphovirus	49107	KC292025	PMID: 23470522	*Clampvirus*	*Madisaviridae*	*Haloarcula hispanica*	*Haloarcula hispanica*	doi.org/10.1016/S0723-2020(86)80152-7
Haloarcula hispanica icosahedral virus 2	HHIV-2	solar saltern, Margherita di Savoia, Italy	icosahedral tailless	30578	JN968479	PMID: 22357274	*Alphasphaerolipovirus*	*Sphaerolipoviridae*	*Haloarcula hispanica*	*Haloarcula hispanica*	doi.org/10.1016/S0723-2020(86)80152-7
SH1	SH1	saline Serpentine Lake, Australia	icosahedral tailless	30889	AY950802	PMID: 15823603	*Alphasphaerolipovirus*	*Sphaerolipoviridae*	*Haloarcula hispanica*	*Haloarcula hispanica*	doi.org/10.1016/S0723-2020(86)80152-7
Haloarcula californiae icosahedral virus 1	HCIV-1	solar saltern, Samut Sakhon, Thailand	icosahedral tailless	31314	KT809302	PMID: 25866903	*Alphasphaerolipovirus*	*Sphaerolipoviridae*	*Haloarcula californiae*	*Haloarcula californiae*	PMID: 6286602

Haloferax strains used to detect growth inhibition zones (potential halocins)																												
H26		**s5a-1**		**SP10-1**		**SS9-6**		**SS10-6**		**SS10-7**		**LR1-5**		**LR1-14**		**LR1-18**		**LR1-19**		**LR1-24**		**LR2-5**		**LR2-16**		***H.mediterranei***	
10^0	10^-2	10^0	10^-2	10^0	10^-2	10^0	10^-2	10^0	10^-2	10^0	10^-2	10^0	10^-2	10^0	10^-2	10^0	10^-2	10^0	10^-2	10^0	10^-2	10^0	10^-2	10^0	10^-2	10^0	10^-2
-	-	-	-	-	-	-	-	-	-	-	-	-	-	+	-	-	-	+	-	+	-	-	-	+	-	-	-
-	-	-	-	-	-	-	-	-	-	-	-	-	-	-	-	-	-	+	-	+	-	-	-	+	-	-	-
-	-	-	-	-	-	-	-	-	-	+	-	-	-	+	-	-	-	-	-	+	-	+	-	+	-	-	-
-	-	-	-	-	-	-	-	-	-	-	-	-	-	-	-	-	-	-	-	-	-	-	-	-	-	-	-
-	-	+	+	-	-	-	-	-	-	+	+	-	-	+	-	-	-	-	-	+	-	-	-	+	-	-	-
-	-	-	-	-	-	-	-	-	-	-	-	-	-	-	-	-	-	-	-	-	-	-	-	-	-	-	-
-	-	-	-	-	-	+	-	-	-	+	-	-	-	+	-	-	-	-	-	+	-	-	-	+	-	-	-
-	-	-	-	-	-	-	-	-	-	-	-	-	-	-	-	-	-	-	-	-	-	+	+	-	-	-	-
-	-	-	-	-	-	-	-	-	-	+	-	-	-	+	-	-	-	-	-	+	-	+	-	+	-	-	-
-	-	-	-	-	-	-	-	-	-	-	-	-	-	+	-	-	-	-	-	-	-	+	-	+	-	-	-
-	-	-	-	-	-	+	-	-	-	+	-	-	-	+	-	-	-	-	-	+	-	+	-	+	-	-	-
-	-	-	-	-	-	-	-	-	-	+	-	-	-	+	-	+	-	+	-	+	-	+	-	+	-	-	-
-	-	-	-	-	-	+	-	-	-	-	-	-	-	+	-	-	-	+	-	+	-	+	-	+	-	-	-
-	-	-	-	-	-	+	-	-	-	-	-	-	-	+	-	-	-	+	-	-	-	-	-	+	-	+	-
-	-	-	-	-	-	-	-	-	-	+	-	-	-	+	-	-	-	-	-	+	-	+	-	+	-	-	-
-	-	-	-	-	-	-	-	-	-	-	-	-	-	-	-	-	-	+	-	+	-	-	-	+	-	-	-
-	-	-	-	-	-	-	-	-	-	+	-	-	-	+	-	-	-	-	-	-	-	-	-	-	-	+	-
-	-	+	+	-	-	-	-	-	-	-	-	-	-	-	-	-	-	-	-	-	-	-	-	-	-	-	-
-	-	-	-	-	-	-	-	-	-	-	-	-	-	-	-	-	-	-	-	-	-	-	-	-	-	-	-

Virus name	Virus abbreviation	Virus origin	Morphotype	Genome length (bp, nt)	Genome Acc. No.	Reference for virus	*Genus*	*Family*	*Isolation host*	*Host used in this study*	Reference for host used
Haloarcula hispanica pleomorphic virus 1	HHPV-1	solar saltern, Margherita di Savoia, Italy	pleomorphic	8082	GU321093	PMID: 20089654	*Alphapleolipovirus*	*Pleolipoviridae*	*Haloarcula hispanica*	*Haloarcula hispanica*	doi.org/10.1016/S0723-2020(86)80152-7
Halorubrum pleomorphic virus 1	HRPV-1	solar saltern, Trapani, Italy	pleomorphic	7048	FJ685651	PMID: 19298373	*Alphapleolipovirus*	*Pleolipoviridae*	*Halorubrum* sp. PV6	*Halorubrum* sp. PV6	PMID: 19298373
Halorubrum pleomorphic virus 2	HRPV-2	solar saltern, Samut Sakhon, Thailand	pleomorphic	10656	JN882264	PMID: 22003883	*Alphapleolipovirus*	*Pleolipoviridae*	*Halorubrum* sp. SS5-4	*Halorubrum* sp. SS7-4	PMID: 22357279
Halorubrum pleomorphic virus 6	HRPV-6	solar saltern, Samut Sakhon, Thailand	pleomorphic	8549	JN882266	PMID: 22003883	*Alphapleolipovirus*	*Pleolipoviridae*	*Halorubrum* sp. SS7-4	*Halorubrum* sp. SS7-4	PMID: 22357279
Halogeometricum pleomorphic virus 1	HGPV-1	Cabo de Gata, Spain	pleomorphic	9694	JN882267	PMID: 22003883	*Betapleolipovirus*	*Pleolipoviridae*	*Halogeometricum* sp. CG-9	*Halogeometricum* sp. CG-9	PMID: 22003883
Haloarcula hispanica pleomorphic virus 3	HHPV-3	solar saltern, Samut Sakhon, Thailand	pleomorphic	11648	KX344510	PMID: 27632564	*Betapleolipovirus*	*Pleolipoviridae*	*Haloarcula hispanica*	*Haloarcula hispanica*	doi.org/10.1016/S0723-2020(86)80152-7
Haloarcula hispanica pleomorphic virus 4	HHPV-4	culture supernatant of Haloferax sp. s5a–1 on Har. Hispanica	pleomorphic	15010	KY264020	PMID: 29495629	*Betapleolipovirus*	*Pleolipoviridae*	*Haloarcula hispanica*	*Haloarcula hispanica*	doi.org/10.1016/S0723-2020(86)80152-7
Halorubrum pleomorphic virus 3	HRPV-3	saline water, Sedom Ponds, Israel	pleomorphic	8770	JN882265	PMID: 22003883	*Betapleolipovirus*	*Pleolipoviridae*	*Halorubrum* sp. SP3-3	*Halorubrum* sp. SP3-3	PMID: 22003883
Halorubrum pleomorphic virus 9	HRPV-9	culture supernatant of Halorubrum sp. B2–2 on Hrr. sp. SS5-4	pleomorphic	16159	KY965934	PMID: 29772256	*Betapleolipovirus*	*Pleolipoviridae*	*Halorubrum* sp. SS5-4	*Halorubrum* sp. SS7-4	PMID: 22357279
Halorubrum pleomorphic virus 10	HRPV10	saline lake Retba, Cape Verde Peninsula, Senegal	pleomorphic	9296	MG550111	PMID: 30920125	*Betapleolipovirus*	*Pleolipoviridae*	*Halorubrum* sp. LR2-17	*Halorubrum* sp. LR2-17	PMID: 30920125
Halorubrum pleomorphic virus 11	HRPV11	saline lake Retba, Cape Verde Peninsula, Senegal	pleomorphic	9368	MG550113	PMID: 30920125	*Betapleolipovirus*	*Pleolipoviridae*	*Halorubrum* sp. LR2-12	*Halorubrum* sp. LR2-12	PMID: 30920125
Halorubrum pleomorphic virus 12	HRPV12	saline lake Retba, Cape Verde Peninsula, Senegal	pleomorphic	9944	MG550110	PMID: 30920125	*Betapleolipovirus*	*Pleolipoviridae*	*Halorubrum* sp. 1-23	*Halorubrum* sp. LR1-23	PMID: 30920125
His2	His2	Pink Lakes, Victoria, Australia	pleomorphic	16067	AF191797	PMID: 16530800	*Gammapleolipovirus*	*Pleolipoviridae*	*Haloarcula hispanica*	*Haloarcula hispanica*	doi.org/10.1016/S0723-2020(86)80152-7
His1	His1	Avalon saltern, Victoria, Australia	spindle-shaped	14462	AF191796	PMID: 9765495	*Salterprovirus*	*Halspiviridae*	*Haloarcula hispanica*	*Haloarcula hispanica*	doi.org/10.1016/S0723-2020(86)80152-7
Halorubrum head-tail virus 1	HRTV-1	solar saltern, Margherita di Savoia, Italy	myovirus	nd	nd	PMID: 22003883	*nd*	*nd*	*Halorubrum* sp. s1-1	*Halorubrum* sp. s1-1	PMID: 23765723
Halorubrum head-tail virus 3	HRTV-3	solar saltern, Margherita di Savoia, Italy	myovirus	nd	nd	PMID: 22003883	*nd*	*nd*	*Halorubrum* sp. S5a-2	*Halorubrum* sp. s5a-2	PMID: 22003883
Halorubrum head-tail virus 6	HRTV-6	solar saltern, Margherita di Savoia, Italy	myovirus	nd	nd	PMID: 22003883	*nd*	*nd*	*Halorubrum* sp. s5a-4	*Halorubrum* sp. s5a-4	PMID: 22003883
Halophilic head-tail virus 1	HTV-1	Eilat, Israel	myovirus	nd	nd	PMID: 22003883	*nd*	*nd*	Halophilic isolate E200-7	Halophilic isolate E200-7	PMID: 22003883
Haloarcula californiae tailed virus 14	HCTV-14	solar saltern, Samut Sakhon, Thailand	myovirus	nd	nd	PMID: 25866903	*nd*	*nd*	*Haloarcula californiae*	*Haloarcula californiae*	PMID: 6286602

Haloferax strains used to detect growth inhibition zones (potential halocins)

H26		s5a-1		SP10-1		SS9-6		SS10-6		SS10-7		LR1-5		LR1-14		LR1-18		LR1-19		LR1-24		LR2-5		LR2-16		*H.mediterranei*	
10^0	10^-2	10^0	10^-2	10^0	10^-2	10^0	10^-2	10^0	10^-2	10^0	10^-2	10^0	10^-2	10^0	10^-2	10^0	10^-2	10^0	10^-2	10^0	10^-2	10^0	10^-2	10^0	10^-2	10^0	10^-2
-	-	-	-	-	-	-	-	-	-	-	-	-	-	-	-	-	-	-	-	-	-	-	-	+	-	-	-
-	-	-	-	-	-	-	-	-	-	-	-	-	-	-	-	-	-	-	-	-	-	-	-	-	-	-	-
-	-	-	-	-	-	-	-	-	-	+	-	-	-	+	-	+	-	+	-	+	-	+	-	+	-	-	-
-	-	-	-	-	-	-	-	-	-	-	-	-	-	-	-	-	-	-	-	-	-	-	-	+	-	-	-
-	-	+	-	-	-	-	-	-	-	+	-	-	-	-	-	-	-	-	-	-	-	+	-	-	-	+	-
-	-	-	-	-	-	-	-	-	-	-	-	-	-	-	-	-	-	-	-	+	-	-	-	+	-	-	-
-	-	-	-	-	-	-	-	-	-	-	-	-	-	-	-	-	-	-	-	+	-	-	-	+	-	-	-
-	-	+	-	-	-	-	-	-	-	-	-	-	-	-	-	-	-	-	-	-	-	-	-	-	-	-	-
-	-	-	-	-	-	-	-	-	-	-	-	-	-	-	-	-	-	-	-	+	-	-	-	+	-	-	-
-	-	-	-	-	-	-	-	-	-	-	-	-	-	-	-	-	-	-	-	-	-	+	+	-	-	-	-
-	-	-	-	-	-	-	-	-	-	-	-	-	-	-	-	-	-	-	+	-	-	+	+	-	-	-	-
-	-	-	-	-	-	-	-	-	-	-	-	-	-	-	-	-	-	-	-	-	-	+	+	-	-	-	-
-	-	-	-	-	-	-	-	-	-	-	-	-	-	-	-	-	-	-	-	-	-	-	-	+	-	-	-
-	-	-	-	-	-	-	-	-	-	-	-	-	-	-	-	-	-	-	-	-	-	-	-	-	-	-	-
-	-	+	+	-	-	-	-	-	-	-	-	-	-	-	-	-	-	-	-	+	+	-	-	-	-	-	-
-	-	-	-	-	-	-	-	-	-	-	-	-	-	-	-	-	-	-	-	-	-	-	-	-	-	-	-
+	+	-	-	-	-	+	+	-	-	+	+	-	-	-	-	-	-	-	-	-	-	-	-	-	-	+	+
-	-	+	-	-	-	-	-	-	-	-	-	-	-	-	-	-	-	-	-	-	-	+	+	-	-	-	-
-	-	-	-	+	+	-	-	-	-	-	-	-	-	-	-	-	-	+	-	+	-	+	-	-	-	-	-

Virus name	Virus abbreviation	Virus origin	Morphotype	Genome length (bp, nt)	Genome Acc. No.	Reference for virus	*Genus*	*Family*	*Isolation host*	*Host used in this study*	Reference for host used
Haloarcula californiae tailed virus 17	HCTV-17	solar saltern, Samut Sakhon, Thailand	siphovirus	nd	nd	PMID: 25866903	*nd*	*nd*	*Haloarcula californiae*	*Haloarcula californiae*	PMID: 6286602
Halorubrum pleomorphic virus 7	HRPV-7	solar saltern, Samut Sakhon, Thailand	pleomorphic	nd	nd	PMID: 25866903	*nd*	*nd*	*Halorubrum* sp. SS5-4	*Halorubrum* sp. SS7-4	PMID: 22357279
Halorubrum pleomorphic virus 8	HRPV-8	solar saltern, Samut Sakhon, Thailand	pleomorphic	nd	nd	PMID: 25866903	*nd*	*nd*	*Halorubrum* sp. SS7-4	*Halorubrum* sp. SP3-3	PMID: 22003883
Haloarcula pleomorphic virus 1	HAPV-1	solar saltern, Samut Sakhon, Thailand	pleomorphic	nd	nd	PMID: 25866903	nd	nd	*Haloarcula* sp. SS13-14	*Haloarcula* sp. SS13-14	PMID: 25866903
nd	Virus isolate 6 (2012)	solar saltern, Margherita di Savoia, Italy	nd	nd	nd	PMID: 22003883	nd	nd	*Halorubrum* sp. s5a-2	*Halorubrum* sp. SS5-7	PMID: 22003883
nd	Virus isolate 17 (2012)	solar saltern, Margherita di Savoia, Italy	nd	nd	nd	PMID: 22003883	nd	nd	*Haloarcula vallismortis*	*Haloarcula vallismortis*	PMID: 667737
nd	Virus isolate 19 (2012)	solar saltern, Margherita di Savoia, Italy	nd	nd	nd	PMID: 22003883	nd	nd	*Haloarcula vallismortis*	*Haloarcula vallismortis*	PMID: 667737
nd	Virus isolate 21 (2012)	solar saltern, Margherita di Savoia, Italy	nd	nd	nd	PMID: 22003883	nd	nd	*Haloarcula vallismortis*	*Haloarcula vallismortis*	PMID: 667737
nd	Virus isolate 23 (2012)	solar saltern, Margherita di Savoia, Italy	nd	nd	nd	PMID: 22003883	nd	nd	*Halorubrum* sp. s1-1	*Halorubrum* sp. s1-1	PMID: 23765723
nd	Virus isolate 24 (2012)	solar saltern, Margherita di Savoia, Italy	nd	nd	nd	PMID: 22003883	nd	nd	*Halorubrum* sp. s1-1	*Halorubrum* sp. s1-1	PMID: 23765723
nd	Virus isolate 26 (2012)	solar saltern, Samut Sakhon, Thailand	nd	nd	nd	PMID: 22003883	nd	nd	*Halorubrum sodomense*	*Halorubrum sodomense*	doi.org/10.1099/00207713-33-2-381
nd	Virus isolate 37 (2015)	solar saltern, Samut Sakhon, Thailand	nd	nd	nd	PMID: 25866903	nd	nd	*Halorubrum sodomense*	*Halorubrum sodomense*	doi.org/10.1099/00207713-33-2-381
nd	Virus isolate 38 (2012)	Eilat, Israel	nd	nd	nd	PMID: 22003883	nd	nd	*Halorubrum sodomense*	*Halorubrum sodomense*	doi.org/10.1099/00207713-33-2-381
nd	Virus isolate 39 (2015)	solar saltern, Samut Sakhon, Thailand	nd	nd	nd	PMID: 25866903	nd	nd	*Halorubrum sodomense*	*Halorubrum sodomense*	doi.org/10.1099/00207713-33-2-381
nd	Virus isolate 40 (2015)	solar saltern, Samut Sakhon, Thailand	nd	nd	nd	PMID: 25866903	nd	nd	*Halorubrum sodomense*	*Halorubrum sodomense*	doi.org/10.1099/00207713-33-2-381
nd	Virus isolate 41 (2012)	Eilat, Israel	nd	nd	nd	PMID: 22003883	nd	nd	*Haloarcula japonica*	*Haloarcula japonica*	doi.org/10.1016/S0723-2020(11)80165-7
nd	Virus isolate 42 (2015)	solar saltern, Samut Sakhon, Thailand	nd	nd	nd	PMID: 25866903	nd	nd	*Halorubrum sodomense*	*Halorubrum sodomense*	doi.org/10.1099/00207713-33-2-381
nd	Virus isolate 43 (2015)	solar saltern, Samut Sakhon, Thailand	nd	nd	nd	PMID: 25866903	nd	nd	*Halorubrum sodomense*	*Halorubrum sodomense*	doi.org/10.1099/00207713-33-2-381
nd	Virus isolate 44 (2015)	solar saltern, Samut Sakhon, Thailand	nd	nd	nd	PMID: 25866903	nd	nd	*Haloarcula japonica*	*Haloarcula japonica*	doi.org/10.1016/S0723-2020(11)80165-7
nd	Virus isolate 45 (2012)	Eilat, Israel	nd	nd	nd	PMID: 22003883	nd	nd	*Halorubrum* sp. E301-4	*Halorubrum* sp. E301-4	PMID: 22003883

(1) HCTV-7 and HCTV-12 are identical and both tested here; HCTV-7 is in used in the future; (2) HCTV-6 and HCTV-13 are identical and both tested here; HCTV-6 is in used in the future
nd, not determined; Growth inhibition was measured at 37°C in MGM. Both the undiluted (10^0) and 1:100 diluted (10^-2) virus results are shown.
Positive growth inhibition is represented with a plus sign (+). Minus sign (-) indicates that no growth inhibition was seen

Haloferax strains used to detect growth inhibition zones (potential halocins)																												
H26		**s5a-1**		**SP10-1**		**SS9-6**		**SS10-6**		**SS10-7**		**LR1-5**		**LR1-14**		**LR1-18**		**LR1-19**		**LR1-24**		**LR2-5**		**LR2-16**		***H.mediterranei***	
10^0	10^-2	10^0	10^-2	10^0	10^-2	10^0	10^-2	10^0	10^-2	10^0	10^-2	10^0	10^-2	10^0	10^-2	10^0	10^-2	10^0	10^-2	10^0	10^-2	10^0	10^-2	10^0	10^-2	10^0	10^-2
-	-	+	+	-	-	-	-	+	-	+	+	-	-	+	-	-	-	-	-	+	-	-	-	+	-	-	-
-	-	-	-	-	-	-	-	-	-	+	-	-	-	+	-	+	-	+	-	+	-	+	-	+	-	-	-
-	-	-	-	-	-	-	-	-	-	-	-	-	-	-	-	-	-	-	-	-	-	-	-	-	-	-	-
-	-	-	-	-	-	-	-	-	-	-	-	-	-	-	-	-	-	-	-	+	-	-	-	+	-	-	-
-	-	-	-	-	-	+	+	-	-	+	+	-	-	+	-	-	-	+	-	+	-	-	-	+	-	-	-
-	-	-	-	-	-	-	-	-	-	+	-	-	-	+	-	-	-	-	-	+	-	+	-	+	-	-	-
-	-	-	-	-	-	-	-	-	-	-	-	-	-	-	+	-	-	-	-	+	-	+	-	+	-	-	-
-	-	-	-	-	-	-	-	-	-	-	-	-	-	-	-	-	-	-	-	+	-	-	-	-	-	-	-
-	-	-	-	-	-	-	-	-	-	-	-	-	-	-	-	-	-	-	-	+	-	-	-	+	-	-	-
+	+	+	+	-	-	+	+	-	-	+	+	-	-	-	-	-	-	-	-	-	-	-	-	-	-	-	-
-	-	-	-	-	-	-	-	-	-	-	-	-	-	-	-	+	-	+	-	+	-	+	-	+	-	+	-
-	-	-	-	-	-	-	-	-	-	+	-	-	-	-	-	-	-	-	-	+	-	-	-	-	-	-	-
-	-	-	-	-	-	-	-	-	-	-	-	-	-	-	-	+	-	+	-	+	-	+	-	+	-	+	-
-	-	-	-	-	-	-	-	-	-	-	-	-	-	-	-	-	-	-	-	+	-	-	-	-	-	-	-
-	-	-	-	-	-	-	-	-	-	-	-	-	-	-	-	-	-	-	-	-	-	-	-	-	-	-	-
-	-	-	-	-	-	-	-	-	-	-	-	-	-	-	-	-	-	-	-	+	-	+	-	+	-	-	-
-	-	-	-	-	-	-	-	-	-	-	-	-	-	+	-	-	-	-	-	-	-	-	-	-	-	-	-
-	-	-	-	-	-	+	-	-	-	-	-	-	-	+	-	-	-	-	-	-	-	-	-	-	-	-	-
-	-	-	-	-	-	-	-	-	-	-	-	-	-	-	-	-	-	-	-	-	-	-	-	-	-	-	-
-	-	-	-	-	-	-	-	-	-	-	-	-	-	-	-	-	-	-	-	-	+	-	+	-	+	-	-

Supplementary Table S3. Underrepresented palindromic motifs in viral genomes[1]

	CTAG	GATC	AGCT	TGCA	CATG
HFTV1	0.0314	0.0714	0.2252	0.8473	0.9074
HCTV-6	0	0	0	0.2976	0.4192
HCTV-15	0	0	0	0.2976	0.4192
HRTV-11	0	0	0	0.2742	0.3604
HSTV-2	0	0	0	0.3023	0.3638
HRTV-7	0	0	0	0.3291	0.3654
HRTV-2	0	0	0	0.3091	0.3721
HRTV-10	0	0	n	0.2756	0.3855
HRTV-20	0	0	n	0.2959	0.3261
HRTV-18	0	0	n	0.2964	0.3263
HRTV-26	0	0	n	0.2764	0.3341
HRTV-22	0.0067	0	n	0.2707	0.3146
HJTV-1	0	0	n	0.24	0.3905
HRTV-21	0	0	n	0.2565	0.3741
HRTV-5	0	0	n	0.2757	0.3566
HRTV-13	0	0	n	0.2604	0.3638
HRTV-16	0	0	n	0.2811	0.3554
HRTV-9	0	0	n	0.3411	0.3623
HCTV-10	0	0	n	0.2886	0.3382
HCTV-8	0	0	n	0.2886	0.3379
HCTV-7	0	0	n	0.2993	0.3408
HCTV-11	0	0	n	0.2994	0.3412
HCTV-9	0	0	n	0.2991	0.3409

[1] Calculated as Odds Markov values where they are not zero. n represent normal frequencies. Orange color incidates the value 0.

Supplementary Table S4. Manual counting of modified DNA motifs found in the genomes of viruses infecting *Hfx. gibbonsii* LR2-5

	CTAG [1]	GCG**C**TG	**A**YCnnnnnC TTYG	CRA**A**Gnnn nnGRT	CC**A**nnnnnn RTCnC	GnG**A**Ynnn nnnTGG
HFTV-1	2	0	2	0	3	9
HCTV-6	0	41	9	14	6	10
HCTV-15	0	41	9	14	6	10
HRTV-11	0	39	6	15	9	7
HSTV-2	0	37	8	14	8	6
HRTV-7	0	32	6	15	9	5
HRTV-2	0	36	8	15	8	9
HRTV-10	0	12	8	10	5	6
HRTV-20	0	14	11	11	7	6
HRTV-18	0	14	11	11	7	6
HRTV-26	0	16	12	9	7	4
HRTV-22	1	13	13	9	6	5
HJTV-1	0	9	9	10	4	9
HRTV-21	0	13	9	10	3	7
HRTV-5	0	10	5	11	5	7
HRTV-13	0	10	6	11	5	8
HRTV-16	0	10	6	10	2	7
HRTV-9	0	14	5	12	3	9
HCTV-10	0	10	5	10	5	7
HCTV-8	0	10	5	10	5	7
HCTV-7	0	10	6	10	5	7
HCTV-11	0	10	6	10	5	7
HCTV-9	0	10	6	10	5	7

[1]Modified bases are shown in bold. The color range blue to yellow is from a low number of occurrences (0) to a high number of occurrences (>30)

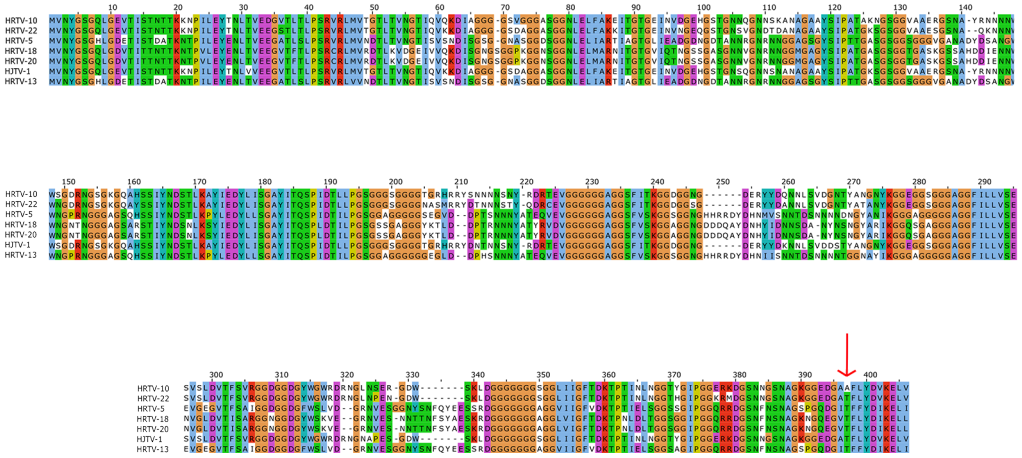

Supplementary Figure S1. Multiple sequence alignment of adhesins belonging to the Group 3

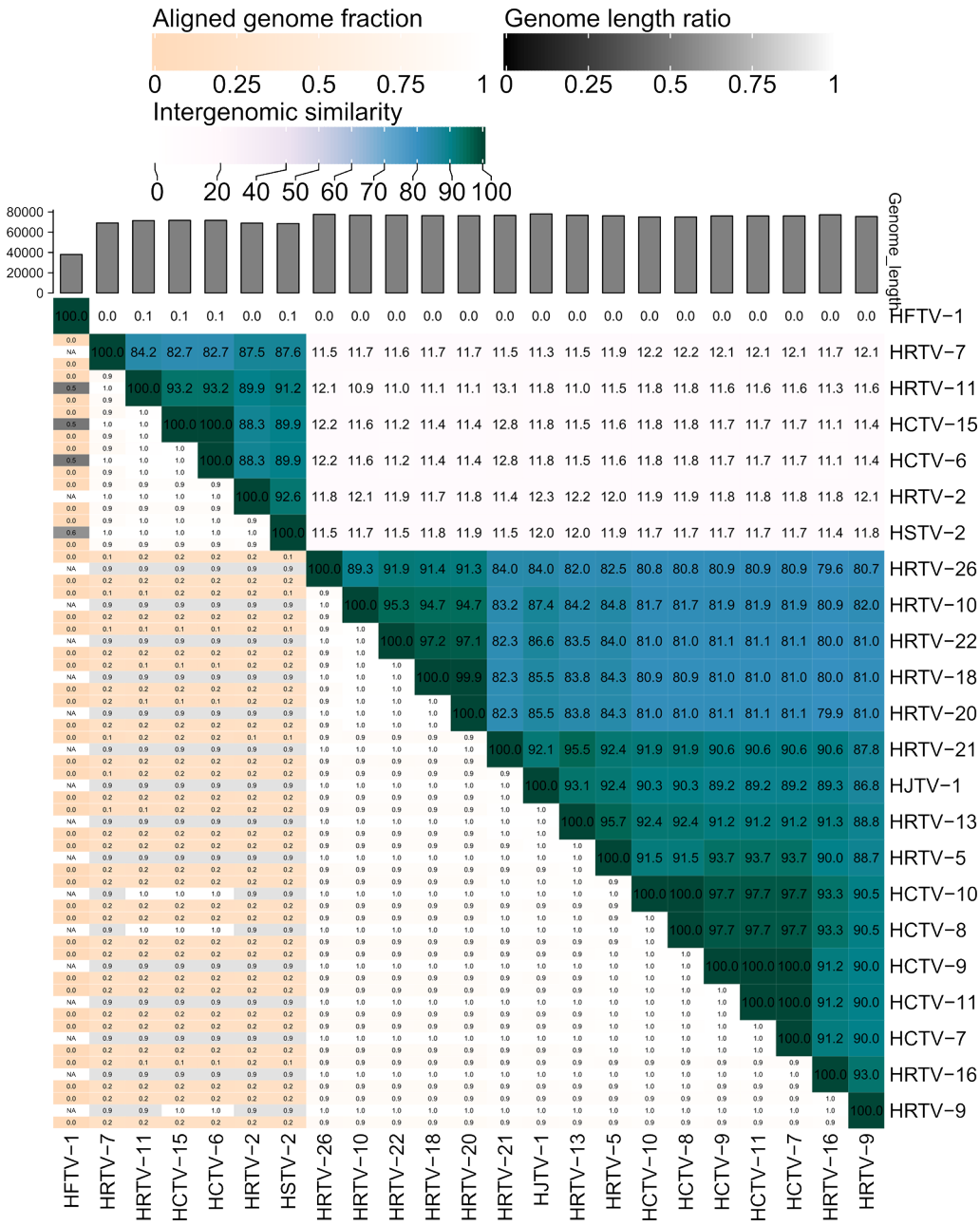

Supplementary Figure S2. VIRIDIC generated heatmap

Supplementary References

1. Allers, T.; Ngo, H.P.; Mevarech, M.; Lloyd, R.G. Development of Additional Selectable Markers for the Halophilic Archaeon Haloferax Volcanii Based on the LeuB and TrpA Genes. *Applied and Environmental Microbiology* **2004**, *70*, 943–953, doi:10.1128/AEM.70.2.943-953.2004.
2. Atanasova, N.S.; Roine, E.; Oren, A.; Bamford, D.H.; Oksanen, H.M. Global Network of Specific Virus-Host Interactions in Hypersaline Environments. *Environmental microbiology* **2012**, *14*, 426–440, doi:10.1111/J.1462-2920.2011.02603.X.
3. Atanasova, N.S.; Demina, T.A.; Buivydas, A.; Bamford, D.H.; Oksanen, H.M. Archaeal Viruses Multiply: Temporal Screening in a Solar Saltern. *Viruses* **2015**, *7*, 1902–1926, doi:10.3390/v7041902.
4. Mizuno, C.M.; Prajapati, B.; Lucas-Staat, S.; Sime-Ngando, T.; Forterre, P.; Bamford, D.H.; Prangishvili, D.; Krupovic, M.; Oksanen, H.M. Novel Haloarchaeal Viruses from Lake Retba Infecting Haloferax and Halorubrum Species. *Environmental Microbiology* **2019**, *21*, 2129–2147, doi:10.1111/1462-2920.14604.
5. Tittes, C.; Schwarzer, S.; Pfeiffer, F.; Dyall-Smith, M.; Rodriguez-Franco, M.; Oksanen, H.M.; Quax, T.E.F. Cellular and Genomic Properties of Haloferax Gibbonsii LR2-5, the Host of Euryarchaeal Virus HFTV1. *Front. Microbiol.* **2021**, *12*, 625599, doi:10.3389/fmicb.2021.625599.
6. Rodriguez-Valera, F.; Juez, G.; Kushner, D.J. Halobacterium Mediterranei Spec, Nov., a New Carbohydrate-Utilizing Extreme Halophile. *Systematic and applied microbiology* **1983**, *4*, 369–381, doi:10.1016/S0723-2020(83)80021-6.